

Abstract

Computational simulations of physical phenomena rely on an accurate discretisation of the model domain. Numerical models have increased in sophistication to a level where it is possible to support terrain-following boundaries that conform accurately to real physical interfaces, and resolve a multiscale of spatial resolutions. Whilst simulation codes are maturing in this area, pre-processing tools have not developed significantly enough to competently initialise these problems in a rigorous, efficient and recomputable manner. In the relatively disjoint field of Geographic Information Systems (GIS) however, techniques and tools for mapping and analysis of geographical data have matured significantly.

If data provenance and recomputability are to be achieved, the manipulation and agglomeration of data in the pre-processing of numerical simulation initialisation data for geophysical models should be integrated into GIS. A new approach to the discretisation of geophysical domains is presented, and introduced with a verified implementation. This brings together the technologies of geospatial analysis, meshing and numerical simulation models. This platform enables us to combine and build up features, quickly drafting and updating mesh descriptions with the rigour that established GIS tools provide. This, combined with the systematic workflow, supports a strong provenance for model initialisation and encourages the convergence of standards.

1 Introduction

Numerical models have increased in sophistication to a point where it is possible to support terrain-following boundaries that conform accurately to real physical interfaces. This enables the accurate simulation of processes of the same scale as boundary features, and with reduced dependence on parameterisations. In structured mesh models, where it is only possible to conform to boundaries in idealised domains, complex boundaries are often approximated by staircase-like surfaces (Griffies et al., 2005).

GMDD

7, 5993–6060, 2014

Integration of GIS into meshing for geophysical models

A. S. Candy et al.

Title Page

Abstract

Introduction

Conclusions

References

Tables

Figures



Back

Close

Full Screen / Esc

Printer-friendly Version

Interactive Discussion



Integration of GIS into meshing for geophysical models

A. S. Candy et al.

Title Page

Abstract

Introduction

Conclusions

References

Tables

Figures



Back

Close

Full Screen / Esc

Printer-friendly Version

Interactive Discussion



Improvements such as partial cells (Pacanowski and Gnanadesikan, 1998; Bernard et al., 2006; Simanjuntak et al., 2009) or shaved cells (Adcroft et al., 1997) mitigate this to a degree with an improved representation of topographically-influenced wave and advective processes. In all cases however, parameterisations are required to ensure boundary conditions are applied correctly and processes close to the boundary behave faithfully (Adcroft and Marshall, 1998). This problem becomes acute for processes whose evolution is heavily influenced by the presence of a boundary, e.g. buoyancy-driven gravity currents that flow along internal isopycnic interfaces or the external domain boundary of the ocean floor (see Legg and Adcroft, 2003).

The importance of representing complex boundaries in the field of marine modelling, to an arbitrary prescribed level of accuracy, is outlined in the review of Griffies et al. (2000). Approaches to faithfully capturing complex boundaries have been investigated with application in the shallow water models TELEMAC (Galland et al., 1991) and the MIKE series of models (DHI Group, 2014), the finite volume model FVCOM (Chen et al., 2003), and the finite element ocean models Fluidity (Pain et al., 2005), ADCIRC coastal model (Westerink et al., 2008), and FESOM (Danilov et al., 2004; Sidorenko et al., 2011). These approaches make it possible for a model to rely less on possibly inconsistent and error-prone parameterisations; instead simulating a larger proportion of the physics of a system.

Whilst simulation codes are maturing in this area, the pre-processing tools have not developed significantly enough to competently constrain problem initialisation for unstructured-mesh models in a rigorous, efficient and reproducible manner. This is necessary to establish provenance of results, where a complete chain is fully specified from pre-processing and initialisation stages to simulation and diagnostics for verification. This ensures the rigorous and auditable testing of scientific software and method, important to maintain public confidence in simulation results and model prediction as highlighted in Farrell et al. (2011).

The complexity of parameter specification in multi-physics models has been tackled through self-validating parameter-comprehensive tools such as Spud (Ham et al.,

Integration of GIS into meshing for geophysical models

A. S. Candy et al.

Title Page

Abstract

Introduction

Conclusions

References

Tables

Figures



Back

Close

Full Screen / Esc

Printer-friendly Version

Interactive Discussion



The GSHHS plugin for Gmsh for example, supports the orientated vector paths available in the GSHHS dataset, developed by Wessel and Smith (1996). Standalone packages such as MeshGUI (Blain et al., 2008) and the River Simulation Tool (Blain et al., 2009) are both built for the ADCIRC coastal model (Westerink et al., 2008). In order to generate two-dimensional unstructured meshes of the Weser estuary of Northern Germany, Zorndt et al. (2012) uses a Matlab tool that interfaces with the BatTri (Bilgili et al., 2006) bathymetry-based grid generator. This approach is combined with ArcGIS (ERSI ArcGIS Platform, 2014) tools for the detection of fixed structures, such as summer dikes. The mature hydrological products from DHI (DHI Group, 2014) such as the MIKE-URBAN, MIKE-FLOOD and MIKE 21 simulation suites contain initialisation tools to import map data and allow editing of coastal and man-made structures. Similarly, the TELEMAC (Galland et al., 1991) numerical shallow water code is initialised with the MATISSE mesh generator program, specifically built as part of the TELEMAC system. As is the case with the other cited examples however, these are limited to specific application scenarios, and also in their interoperability. With these tools it can also be difficult to adjust the workflow in order to make edits or combine datasets, which is often required to make the most of unstructured mesh simulations. Often bespoke scripting is required. A more general tool is required, and ideally one that integrates the two relatively mature fields of mesh generation and GIS.

The remainder of the paper is set out as follows. In Sect. 2, an overview of the challenges faced in the discretisation of geophysical domains is given. Those intrinsic to unstructured mesh construction are described in further detail in Sect. 3. A description of GIS geospatial frameworks and how they are an appropriate platform to build and extend to use in geophysical model initialisation is given in Sect. 4. A specific case study with complex features is introduced here to give context to the described challenges and requirements. Application of geometric constraints to both interfaces and regions of the surface geoid are considered in Sect. 5. Manipulation of source datasets is discussed in Sect. 6, with specific challenges in the assimilation of multiple resources. Finally, we draw conclusions in Sect. 7 and give perspective on future

outlook and demand for this approach. An open source implementation has also been made available.

2 Challenges in domain discretisation for geophysical models

There are many inherent challenges in the preparation of domain boundary representations and element cell size specification in mesh generation. Under geometric constraints, the boundary representation should be orientated, non-intersecting, closed and well-resolved with a smoothness appropriate to local dynamics. The shape and size of mesh elements throughout the domain can be described by a metric tensor field to allow complete generalisation. This should be complete, defined over the whole domain and appropriately-graded to avoid excessive discretisation errors (Pain et al., 2005; Piggott et al., 2005; Gorman et al., 2006).

Discretisation of the domain for a geophysical simulation requires the following:

1. *Accurate representation of boundaries* such that they are contour-following to a degree prescribed by the metric size field, with aligned faces such that forcing data is consistently applied.
2. *Spatial mesh resolution* to minimise error; with efficient aggregation of contributing factors, ease of prototyping and experimentation of metric functions and contributing fields, over the entire extent of the bounded domain.
3. *Accurate geometric specification of regions* and boundary features; to provide for appropriate interfacing of regions of differing physics, model coupling and parameterisation application.
4. *Consistent pre-processing*, such that all contributing source data is handled equally.
5. *Quick to draft and prototype*, such that user time can be focused on high-level development of the physics of the modelled system.

Integration of GIS into meshing for geophysical models

A. S. Candy et al.

Title Page

Abstract

Introduction

Conclusions

References

Tables

Figures



Back

Close

Full Screen / Esc

Printer-friendly Version

Interactive Discussion



Integration of GIS into meshing for geophysical models

A. S. Candy et al.

Title Page

Abstract

Introduction

Conclusions

References

Tables

Figures



Back

Close

Full Screen / Esc

Printer-friendly Version

Interactive Discussion



6. Facilitate the easy manipulation and process integration of *large datasets*.
7. *Hierarchy of automation*, such that individual automated elements of the workflow can be brought down to a lower-level for finer-scale adjustments.
8. *Provenance* to ensure the full workflow from initialisation to simulation and verification diagnostics are reproducible.
9. *Standardisation of interaction* to enable interoperability between both tools and scientists.

In the relatively disjoint field of GIS, techniques and tools for mapping and analysis of geographic data have matured significantly. These tools continue to develop rapidly due to their wide applicability. GIS platforms (see Steiniger and Bocher, 2009, for a description) offer a prototyping stage to combine and build up a range of features from different digital elevation maps (DEMs), contours and constructions. With the proposed approach, these features can be quickly drafted in and the resulting mesh descriptions updated with the rigour that established GIS tools provide. For geospatial data, these tools already interact through established standardised data formats and syntax. These are described and evaluated for open source GIS frameworks in Chen et al. (2010) and under the CASCADOSS (2009) project.

The approach described here seeks to adopt this form of framework for handling and processing information required in the construction of unstructured meshes. This includes information such as the boundary representation, surface fields, region identification and mesh construction process; all of which share a degree of similarity with data already handled by GIS platforms.

Geophysical bounding features are very complex, characterised by fractal-like geometries over a large range of scales. In ocean domains for example, these boundaries include shorelines, the grounding lines where ice meets bedrock, and ocean bathymetry. The analysis of such features has been the focus of much effort in the GIS community, and well-established techniques exist to competently handle the extraction

Integration of GIS into meshing for geophysical models

A. S. Candy et al.

Title Page

Abstract

Introduction

Conclusions

References

Tables

Figures



Back

Close

Full Screen / Esc

Printer-friendly Version

Interactive Discussion



Similarly, this difference in scale motivates the discretisation of the domain in parts. The approach taken to represent the three-dimensional domain is to describe the bounding surfaces that enclose it, in the same way a *B-rep* method is used in CAD models. This is in contrast to the CSG approach described above where the domain is constrained in terms of Boolean operations on primitive objects. First the surface geoid domain is constrained by a boundary representation contour parameterised in two-dimensional space. The full three-dimensional domain is then constrained by two fields defined on the surface geoid that mark the top and bottom domain surfaces. The mesh metric and forcing fields can also be split in this manner. An outline of the processes required to constrain unstructured meshes for geophysical models with regard to the two fundamental components of the geoid boundary representation and fields describing mesh resolution, surface height and forcings are described below.

3.1 Boundary representation

The generation of boundary representations for geophysical models requires:

1. An orientated vector path of the encompassing surface geoid bound defined in two-dimensional parameter space.
2. Height maps defined in the surface geoid domain.

An example of the former for a region containing the British Isles, North Sea and coast-line of northwest Continental Europe is shown in Fig. 1a, under a Universal Transverse Mercator (UTM) projection, using the World Geodetic System (WGS) revision 84, EPSG:4326 ellipsoid, in zone 30U centred on 3° W 52° N. In this zone the central meridian lies at 3° W, (5.00×10^5 m, 5.76×10^6 m) in the coordinates of the projection. The GIS package is used to project all source data to the projection intended for numerical simulation, in order to construct the boundary representation, metric and subsequently the mesh. This projection is applied in all results presented here, unless otherwise noted.

Integration of GIS into meshing for geophysical models

A. S. Candy et al.

Title Page

Abstract

Introduction

Conclusions

References

Tables

Figures



Back

Close

Full Screen / Esc

Printer-friendly Version

Interactive Discussion



For unstructured meshes with conforming boundaries, one challenge is to generate an orientated vector path to a required, spatially variable, level of accuracy in a rigorous and reproducible manner. The representation at the boundary under the freer constraints of an unstructured mesh can be optimised to best represent it given its shape and other local features or focus requirements. This is a relatively new problem, and a challenge in taking full advantage of unstructured mesh models, such as Fluidity (Piggott et al., 2008; Pain et al., 2005), FESOM (Sidorenko et al., 2011) and the ADCIRC coastal model (Westerink et al., 2008).

At initialisation, approaches have been investigated to optimise boundary representation, such as the shoreline optimisation of Gorman et al. (2007), and specific feature treatments, such as the special consideration of channels in meshing highly irregular oceanic archipelagos studied in van Scheltinga et al. (2012), and the modification of an advancing front meshing algorithm to improve the representation of sharp bathymetric features in Mazzolari et al. (2014). The GSHHS plugin (Lambrechts et al., 2008) competently generates ocean coastline boundary representations (see also Legrand et al., 2007) from the pre-prepared orientated GSHHS (Wessel and Smith, 1996) dataset in the syntax of Gmsh (Geuzaine and Remacle, 2009). This process successfully handles the domain initialisation for model problems where the boundaries defined by GSHHS are appropriate. Domains containing modifications to GSHHS-defined boundary representations, such as coastal domains including river estuaries, or tidal ocean simulations including the water masses of the ice shelf cavities of Antarctica for example, are difficult to achieve in a rigorous and reproducible manner. The shoreline and bathymetry optimisation approach implemented in Terreno, built on Gorman et al. (2006, 2007) provides good, optimised constraint on unstructured mesh generation, but is limited by its scope for a hierarchy of automation because it is not integrated into GIS.

These types of approaches are well-suited to a limited subset of geophysical problems, their development was motivated by specific modelling studies rather than an integrated approach. These methods should form a part of the approach embracing the defining points (1)–(9) above in Sect. 2.

3.1.1 Use of vector illustration packages for path manipulation

Tools for manipulating paths (specifically polylines) have long been the focus of vector illustration packages. These now contain robust interfaces that can be applied to boundary representation generation. Interfacing can be achieved by the conversion of path data into a format such as the standardised Scalable Vector Graphics (SVG) data type. This process is adopted in Gourgue et al. (2009), de Brye (2011) and Kärnä et al. (2011), and described in more detail in Lambrechts and Seny (2011). These tools were also used as part of the process of boundary and metric generation in Wells et al. (2010) and further described in Gorman et al. (2008) to generate domains of ancient seas. It is also possible to trace contours in rasters using these vector illustration tools, that can be used to develop boundary representations. Since these tools have not been developed with geographic applications specifically in mind, this approach does not take into account accompanying metadata nor consider the map projection of the input. Care is required to ensure that multiple sources are brought in at the same scaling and projection, and for format translation. Tools exist for path simplification, although not in a geographic context, and not, for example, taking into account any map projections made. Hence path simplification routines that take into account spatial distances will not act correctly in this case. Additionally, hand-editing is limited in its rigour and reproducibility, and soon becomes limited for domains that include a multiscale of features with complex boundaries. This problem will only become more acute as it becomes possible to model more scales concurrently.

The data format most prevalent in vector illustration packages is SVG, which is a fully open standard, making it easy to support interoperability, as opposed to the partly-proprietary Environmental Systems Research Institute (ESRI) shapefile format also in common use (defined by the ESRI, 1998). The suitability of the SVG data format in an open architecture vector GIS tool is evaluated in Dunfey et al. (2006). The specific handling of geospatial metadata alongside the SVG format is considered in Antoniou and Tsoulos (2006) using Geography Markup Language (GML), an eXtensible Markup

Integration of GIS into meshing for geophysical models

A. S. Candy et al.

Title Page

Abstract

Introduction

Conclusions

References

Tables

Figures



Back

Close

Full Screen / Esc

Printer-friendly Version

Interactive Discussion



Integration of GIS into meshing for geophysical models

A. S. Candy et al.

Title Page

Abstract

Introduction

Conclusions

References

Tables

Figures



Back

Close

Full Screen / Esc

Printer-friendly Version

Interactive Discussion



and forcings. Like boundary representation generation, spatial resolution can be defined in two components in the case of a geophysical domain. This allows the consideration of the spatial metric of the surface geoid domain to be developed concurrently with its bounds. The bathymetry field of Fig. 2a illustrates an example two-dimensional field required for the surface geoid metric and height extrusion fields required in the generation of the full boundary representation. In the generation of spatial metrics for geophysical models outlined above, the fundamental data forms required are:

1. Two-dimensional fields complete within the surface geoid.
2. A description of variation of spatial vertical resolution.

The former specifies the spatial resolution horizontally in the surface geoid. The latter could be a function of one-dimensional parameter space, a function of a derived or prognostic variable (such as the density for isopycnic layers), or a full 3-D scalar field.

The meshing tool Gmsh (applied in the initialisation of many of the ocean models introduced in Sect. 1) uses a nearest neighbour algorithm (Arya et al., 1998) to enable metrics based on proximity to domain boundary to be applied. This permits a good geometric boundary representation whilst maintaining a reasonable number of degrees of freedom. This metric is poor in some geometric regions however. In the case of archipelagos, van Scheltinga et al. (2012) have developed a mesh size field which modifies the nearest neighbour algorithm to take into account domain boundaries which lie close to each other. The application of GIS for geospatial analysis of surface water and drainage processes has been extended from averaged bin-based models (such as McKinney and Cai, 2002), to hydrodynamic models. The study of Merwade et al. (2008) develops a domain discretisation of the Brazos River at a meandering bend from airborne LiDAR data and finds that existing GIS tools do not honour river flow direction, provide an unrealistic interpolation of cross sections, and generate a poor representation of the terrain as a result. This leads to the development of techniques for channel-fitted coordinate systems for meshes of river systems.

Integration of GIS into meshing for geophysical models

A. S. Candy et al.

Title Page

Abstract

Introduction

Conclusions

References

Tables

Figures



Back

Close

Full Screen / Esc

Printer-friendly Version

Interactive Discussion



For accurate interfacing of regions in integrated hydrologic models, Heinzer et al. (2012) embeds mesh generation software (Triangle; Shewchuk, 2002) into a GIS platform (here the ERSI ArcGIS Platform, 2014) to implement a feature-constraint mesh generation algorithm based on Douglas and Peucker (1973) with the aim of (like Gorman et al., 2007) optimising bounding line representation. The algorithms presented in Gorman et al. (2006) optimise oceanic bathymetry representation based on metrics of boundary curvature. An algorithm to enhance mesh quality based on an equilibrium spring force balance is presented in Conroy et al. (2012) for improved matrix conditioning during simulation. These techniques are exactly those that can be brought into the generation of the spatial resolution metric, in combination with internal interfaces to guide the positioning of mesh element faces.

In addition to metrics based on topological features, those based on physical properties of the system have also been developed. Gravity waves, for example, which propagate at a speed of \sqrt{gH} with g the acceleration due to gravity and H the ocean depth, can be well-captured with a spatial metric ensuring the Courant condition is satisfied (see Dietrich et al., 2008, for a consideration of mesh refinement based on physical properties).

This highlights that a combination of metrics are often required, particularly in multi-scale multi-physics models, where complex boundaries and dynamics exist. Tools such as those provided in the GMT suite (Wessel and Smith, 1998) can be used to rigorously process and combine these datasets. Although these tools do interact with standard data types and work efficiently on large datasets in a process that is reproducible, manipulation in a GIS framework brings additional benefits. It is easier to manage all model data, and it processes it concurrently in a consistent way. The interface, manipulation of metadata instead of the raw data and on-the-fly transformations (for map projections, for example) make the process faster and more efficient for prototyping and experimenting on initialisation scenarios. It is also possible to use raster fields with a large disparity in resolution and spatial scales, e.g. a global bathymetry dataset with

a spatial resolution of kilometres with a coastal dataset with a resolution on the order of metres. This is demonstrated in the application shown later in Fig. 16.

4 Integration with Geographic Information Systems

In the preparation of maps and for the purpose of geospatial analysis, GIS tools have been well-developed and are adept in the generation of contours from raster fields, and subsequent operations on these. Due to the broad range of methods used to capture and generate geospatial data, and that storage formats and standards have evolved in time, GIS packages are built to handle a wide variety of inputs. Data often requires processing to match formal standards, or editing to ensure it is consistent with other sources; removing known errors, or adjustments to deal with jumps in the spatial resolution in datasets, for example.

The data and associated processing tools in the case of vector types are significantly more complex than the raster case. The latter is inherently structured, representing a surjective function from quadrilateral-based regions to an indexed range of scalar values. Data can be constructed and stored as a matrix form, with processing achieved through matrix operations. Errors introduced in observational measurements, such as out of bound values, can be fixed by minimum and maximum operations on a single cell, or local reconstruction techniques. To ensure data is represented appropriate to its resolution, subsampling, or local binning or smoothing operations on the matrix are applied. Errors from the degradation of source materials may need to be removed by hand, such as flaws in aged maps, or discoloured photographs. The process of digitisation may itself introduce errors that need treatment, such as dirt on a camera lens, or scanner glass. The processing in some of these cases can be automated, with for example interference in remotely sensed data, which can be corrected by assimilation of data from multiple sources. Generally, for raster data, these are relatively simple operations on data in a relatively transparent format.

Integration of GIS into meshing for geophysical models

A. S. Candy et al.

Title Page

Abstract

Introduction

Conclusions

References

Tables

Figures



Back

Close

Full Screen / Esc

Printer-friendly Version

Interactive Discussion



Integration of GIS into meshing for geophysical models

A. S. Candy et al.

Title Page

Abstract

Introduction

Conclusions

References

Tables

Figures



Back

Close

Full Screen / Esc

Printer-friendly Version

Interactive Discussion



Vector data is more complex than its raster counterpart; in its format, range of types, required metadata and overall structure. Additionally, as well as ensuring the vector paths are an accurate representation of geographic features, and optimised with procedures such as the Douglas and Peucker (1973) algorithm, vector data is required to be *topologically correct*. Regions should be fully bounded by polylines that are closed, appropriately oriented and form polygons that are disjoint. Networks should be properly linked, such as in the case of infrastructure and transportation planning, where underground urban pipe systems or road networks must be located correctly to ensure connections are established at junctions, for example. Here we find parallels with the pre-processing steps required for geophysical model initialisation, where a hierarchy of automation and levels of editing are required.

As computational models encompass a larger range of physics and tend towards *system models* (CESM, 2014; Taylor et al., 2012), it is becoming more important to develop and introduce consistent pre-processing approaches, that possess a hierarchy of automation and facilitate the easy manipulation of large datasets. There is the opportunity to learn from observational science and the field of geospatial analysis, to adopt approaches and technology such as GIS, where it is common to combine multiple observational datasets to derive secondary fields for analysis. Working with raster and vector paths in two-dimensional space is exactly what is required for the generation of boundary representations and spatial metrics for geophysical model domains as highlighted above.

GIS tools provide a visual, interactive framework for editing geospatial data. Efficient data management enables editing at a range of scales, to ensure coverage at the large scale and continuity of contours at the fine scale. A visual representation of all of the components contributing to the domain discretisation is essential in achieving consistency, efficient prototyping and integration of large datasets, requirements (4), (5), and (6) of Sect. 2. The projection that geospatial data is stored and presented in is important, and GIS packages can interpret and transform these on-the-fly, so that all components are presented and edited consistently.

Integration of GIS into meshing for geophysical models

A. S. Candy et al.

Title Page

Abstract

Introduction

Conclusions

References

Tables

Figures



Back

Close

Full Screen / Esc

Printer-friendly Version

Interactive Discussion



For model intercomparisons and validation on benchmarks, domains are often described with closures along geometric features or references to particular coordinate systems. For example, parts of domains not bounded by geophysical contours such as a coastline, can be closed along meridians or parallels. A more complicated example is shown in the boundary representation of Fig. 1a, where a function of bathymetry is used to define the bound along the continental shelf break. This is relatively easily reproduced within a GIS framework, where the function of bathymetry can be calculated on a raster of bathymetry, contoured and connected to the coastline boundary which characterises the curvature of the seabed surface.

For model intercomparisons with this approach, data provenance and a consistency between model setups with regard to boundary definition can be achieved through a distribution of shapefiles, or a similar standardised polyline data format accompanied with graphical metadata. This is a physical description of the boundary, at an appropriate fidelity to well-characterise its features for the problem it describes. The discretisation to form a mesh and identification is then up to individual modelling studies, taking into account specific constraint requirements of the simulation approach in question.

Additionally, the standardised data formats used facilitate the distribution and interpretation of this data to other scientists and researchers for comparative studies. The conventions for climate and forecast (CF) metadata (Gregory, 2003a) are designed to promote the processing and sharing of geophysical spatial data. The CF conventions are increasingly gaining acceptance and have been adopted by a number of projects and groups as a primary standard. The conventions define metadata that provide a definitive (“self-describing”) description of what the data in each variable represents, and the spatial and temporal properties of the data. This enables users of data from different sources to decide which quantities are comparable, and facilitates building applications with powerful extraction, re-gridding, diagnostic and display capabilities. These conventions are implemented on top of a storage layer data format, such as the Network Common Data Form (NetCDF Rew et al., 2014), which is open, platform-independent and an efficient format to access and process array-orientated

scientific data (Eaton et al., 2008; Gregory, 2003b). The latest revision of the standard netCDF-4, allows the use of the HDF5 (Hierarchical Data Format, HDF5, 2014) data format, which is hierarchical with B-trees (Comer, 1979) for efficient indexing of both array and non-array data. These standards form part of the Open Geospatial Consortium (OGC, 2014) and build on older standards such as the GeoTIFF (Ritter and Ruth, 1997) format commonly used by GIS tools. GeoTIFF extended the standard TIFF format to allow georeferencing information to be embedded within the header, to include details of the map projection, coordinate system, ellipsoid and datums, to provide a complete description in order to establish the exact spatial reference for the data.

Vector data is standardised by the commonly-used Environmental Systems Research Institute (ESRI) shapefile format (defined by ESRI, 1998). Shapefile versions of the GSHHS datasets exist and make it possible that a GIS tool could replace the function of the GSHHS Gmsh plugin, allowing the generation of boundary representations based on the prepared GSHHS coastlines, but also their editing and combination with other data sources, as is demonstrated in Fig. 1a.

GIS tools offer a framework for geophysical model initialisation satisfying the required points (1)–(9) listed above in Sect. 2. Treatments for specific cases such as the Gmsh GSHHS plugin (Lambrechts et al., 2008), shoreline optimisation (Gorman et al., 2007), archipelagos (van Scheltinga et al., 2012) can be integrated through the extensible support in GIS packages, such as the PyQGIS Python interface (PyQGIS, 2014) available in the Quantum GIS (GIS Quantum GIS Development Team, 2012; Sherman, 2008) package. It is noteworthy that the Gmsh GSHHS plugin and the shoreline and bathymetry optimisation code of the Terreno Project (2013) are no longer supported. This highlights the need to integrate these features into community codes in order to be sustainable. There is a demand for a general approach that supports a hierarchy of automation, that importantly, invokes a standardisation of interaction, interfacing with standard data formats to ensure interoperability.

The approach presented here has been facilitated by an implementation coupling GIS, meshing and simulation tools. The QGIS package was chosen due to its adoption

GMDD

7, 5993–6060, 2014

Integration of GIS into meshing for geophysical models

A. S. Candy et al.

Title Page

Abstract

Introduction

Conclusions

References

Tables

Figures



Back

Close

Full Screen / Esc

Printer-friendly Version

Interactive Discussion



Integration of GIS into meshing for geophysical models

A. S. Candy et al.

Title Page

Abstract

Introduction

Conclusions

References

Tables

Figures



Back

Close

Full Screen / Esc

Printer-friendly Version

Interactive Discussion



of open standards (Steiniger and Hunter, 2013), the evaluation of (Chen et al., 2010; CASCADOSS, 2009), and access to internal functions through a comprehensive API. Development of QGIS capability has been significantly driven by user contributions through its plugin architecture. QGIS already relies on well-regarded libraries for geometric operations, such as GDAL (Geospatial Data Abstraction Library, 2014) and GMT (Wessel and Smith, 1998) for raster manipulations, NetCDF (Rew et al., 2014) for raster storage, shapefiles for vector storage, PROJ.4 (Cartographic Projections Library, 2014) for projections and GRASS (Neteler et al., 2012; Geographic Resources Analysis Support System, 2014), a general GIS library. Several plugins have been developed to implement the coupling. These are written in Python (Python Software Foundation, 2011) and interact with QGIS through its plugin architecture and exposed modules in PyQGIS. Additional algorithms from CGAL (The CGAL Project, 2013) are also used to provide fast, efficient and accurate vector operations.

4.1 Application case study: Portland Harbour and Chesil Beach

We now focus on an application case within a GIS framework, choosing a familiar environment for a GIS study, such that it is on a scale typically considered with GIS tools, using data designed for GIS manipulation. Additional, less conventional datasets are introduced and discussed in Sect. 6. The region of interest selected lies on the south coast of the UK (highlighted in Fig. 4a), centred around Portland Harbour, the town of Weymouth and the tied Isle of Portland. An image of the region is shown in Fig. 4b with bounds $[-2.71, -2.22] \times [50.45, 50.74]$, for longitude-latitude coordinates (ψ, ϕ) . In this example, we will work towards a discretisation of the water-filled regions of the domain, with the aim of preparing the initialisation data required for a simulation code solving fluid dynamics equations such as the Navier–Stokes (e.g. Fluidity Piggott et al., 2008) or shallow-water (e.g. Galland et al., 1991; White et al., 2008) systems.

Although the application is common in a GIS setting, the region contains a range of interesting geological and man-made features that pose a challenge to mesh with existing tools. It is not only a challenge to characterise the region accurately, without

Integration of GIS into meshing for geophysical models

A. S. Candy et al.

Title Page

Abstract

Introduction

Conclusions

References

Tables

Figures



Back

Close

Full Screen / Esc

Printer-friendly Version

Interactive Discussion



automated tools it is a slow, laborious and error-prone task. The site is part of the Jurassic Coast, an UNESCO World Heritage Site, and is itself of great scientific interest. In particular, it has been shown (in for example Bastos et al., 2003) that the shape of the Isle of Portland coastline and bathymetric features in the region have a strong influence on local tidal flow, the development of eddies and dispersion of sediment. In Bastos et al. (2003), tidal flow around the headland is modelled and the distinct morphology is found to generate transient tidal eddies which are responsible for the net bedload transport of sand at the seabed. Sediment dispersion is dominated by these ebbing flows rather than a background current. An accurate and appropriate representation of the characteristic morphology of the region is critical in order to model the transient tidal flows and the resultant bed shear stress, if sediment dispersion is to be captured well. This makes it exactly the type of problem that demands the initialisation approach described here.

The high tidal stream velocities around the headland and relative close proximity to population centres mean the region is a promising site for tidal stream energy exploitation, which is investigated in Blunden and Bahaj (2006). Like the Bastos et al. (2003) study, this develops a model of tidal flows using the TELEMAC (Galland et al., 1991) numerical shallow water code. This is initialised with the MATISSE mesh generator program, specifically built as part of the TELEMAC system.

The selected example domain contains the following range of characteristic features in the two-dimensional geoid surface:

- A *fractal-like coastline*.
- *Small-scale natural features* along the coast, such as Lulworth Cove.
- An *isle* off of the mainland connected by a *thin spit*.
- A thin, steep-banked tombolo-like *shingle barrier beach*.
- A brackish coastal *fleet lagoon*.

- The lagoon is connected to the open waters by a *bridged thin channel*.
- *Portland Harbour*, the second largest man-made harbour in the world.
- Many relatively *small-scale man-made structures* built around the harbour.
- Man-made coastal defences.

5 The shingle Chesil Beach (shown in Fig. 4 and seen in Fig. 17) is 29 km long, and shelters the Fleet, a shallow tidal lagoon that runs from Abbotsbury in the northwest down to the village of Chiswell at its eastern end, where it is connected to open waters by a small channel under Ferry Bridge. The beach is 200 m wide and 15 m high and acts as a natural defence from hurricanes and storm surges for Weymouth, Portland Har-

10 bour and the surrounding villages such as Chiswell. The material for the shingle beach is largely debris from Upper Greensand chert from the erosion of cliffs at Lyme Bay to the west. Human activity in West Bay of Bridport means there is now no resupply (Bray, 1992) and losses from the natural barrier can be seen in washover fans (see Fig. 17). Without intervention, the beach will be eroded and destroyed in a similar process to

15 that of the smaller Hurst Spit to the east. Man-made defensive structures have been build on the exposed western side of the beach to protect the populated regions. Chesil Beach openly faces the Atlantic Ocean and is occasionally subject to large waves and significant storm surges, the remnants of Atlantic hurricanes. These surges have over-

20 washed the bank in the past and flooded Chesil village, notably in 1703 (Defoe, 1703) and 1824 (Le Pard, 1999) when there was huge destruction. In early 2014, the UK sustained serious coastal damage, widespread and persistent flooding; the culmination of an exceptional run of winter storms (Met Office, 2014). In Portland, sea defences were overcome and residents evacuated. The natural barrier of Chesil Beach itself has been reshaped by the huge waves (The Guardian, 2014), and will take years to recover.

25 Fig. 6 shows the region with data from *Ordnance Survey (OS)*, the national mapping agency of Great Britain. The underlying raster is the *OS Street View* product, publicly available since April 2010 as part of the OS OpenData (2013) initiative, certified as

Integration of GIS into meshing for geophysical models

A. S. Candy et al.

Title Page

Abstract

Introduction

Conclusions

References

Tables

Figures



Back

Close

Full Screen / Esc

Printer-friendly Version

Interactive Discussion



open access by the Open Data Institute (ODI, 2014). This is a 1 : 10 000 scale, street-level, colour, digital raster mapping (in a GeoTIFF, TIFF-LZW format), split into tiles that have been specifically designed for manipulation with GIS tools. The tiles used in this study are 5 km × 5 km in size and part of the National Grid Reference 100 km × 100 km square “SY” collection. The outlined vector path defining the tidal water boundary is provided by *OS VectorMap District*, another product available from *OS OpenData*. This is an ESRI shapefile broken up into the same sized tiles, and again, the “SY” collection is used here.

Using GIS tools for vector manipulation, the separate tiles of *OS VectorMap District* are combined into a single layer, multi-part vector. The separate paths are first brought into a single layer (and hence single shapefile) using a union operation. This is followed by a “dissolve” to eliminate paths internal to the regions (e.g. including those following tile boundaries). The result is a multi-part vector path marking the tidal boundary of the mainland and individual bodies of land, such as part of the man-made harbour constructs pictured in Fig. 14, more clearly seen in the zoomed in section of the domain in Fig. 7b.

At this point, finer-scale operations to prepare the domain for the specific application required are easily facilitated with a GIS interface. Here the fleet lagoon is a separate body of water, and for simulation we require a continuous simply-connected domain in the two-dimensional surface geoid. The tidal boundary in the *OS VectorMap District* dataset has been closed by Ferry Bridge at the mouth of fleet Lagoon. The fleet can be removed and the tidal boundary left extending up to the bridge by simply removing the path enclosing the lagoon. Alternatively, to open up the lagoon, a contour of the *OS Street View* raster is first taken in GIS, to identify the man-made structure of the bridge. In order to remove the bridge, this contour is then used, through a polygon union operation, to join up the two vector paths, and connect the waters. Finer-scale path intersection tools and hand-editing of the joins are made in the GIS interface to ensure the boundary representation is an accurate representation of the mapped boundary. The result is shown in Fig. 7a, highlighted by a black circle. Using a GIS package

GMDD

7, 5993–6060, 2014

Integration of GIS into meshing for geophysical models

A. S. Candy et al.

Title Page

Abstract

Introduction

Conclusions

References

Tables

Figures



Back

Close

Full Screen / Esc

Printer-friendly Version

Interactive Discussion



facilitates this editing in a fast, easy-to-prototype and rigorous process; assimilating data from various sources.

Combined with a vector drawn to outline the bounding box of the whole region, the produced path defines a closed polygon that outlines the land, as defined by the tidal boundary. Using the GIS interface and tools, it is trivial to produce a polygon defining the fluid-filled domain using a vector subtraction. The two developed vector layers marking the land and sea are shown in Fig. 9.

4.2 Geometric constraint of boundary features

In order to apply boundary conditions and constrain geometric features on the boundary representation, it is necessary to further divide the established paths. In the case of a fluid dynamics simulation in the domain introduced above, it is common to apply different boundary conditions to the coastline and open ocean. These boundaries originate from different vector sources. In the example case, the coastline boundary is a modified *OS VectorMap District* polyline and the open boundary a bounding box encompassing the whole region. When the intersection is made, a point is placed at the intersection, and it is then easy to mark the paths either side with different identification labels. In other cases it is necessary to add points to the path to ensure the boundaries are identified correctly.

In the boundary representation, the two distinct parts identified as coastline and open boundaries respectively, are grouped separately and when meshed, their representation optimised independently in order to constrain this point of intersection that marks a transition of physical properties along the path. This ensures the intersection appears and is maintained in the output mesh, for whichever metric is provided to guide the optimisation of the mesh boundary representation.

This approach is also used to constrain geometric features in the boundary representation. Key parts of man-made structures or key geometric features under study can be forced to appear in the output mesh. For a flux prescribed for a river outflow at the boundary, or a run-off model, the river opening can be ensured to have an accurate

Integration of GIS into meshing for geophysical models

A. S. Candy et al.

Title Page

Abstract

Introduction

Conclusions

References

Tables

Figures



Back

Close

Full Screen / Esc

Printer-friendly Version

Interactive Discussion



representation in the output mesh by ensuring the two points at either side of the river opening appear in the output mesh boundary. These types of geometric constraints are easy to introduce in a GIS framework, rigorously guided by mapping inputs.

5 Geometric constraint of internal interfaces and regions

5 Definition and identification of the boundary representation has been established above using GIS tools, to give an accurate representation through a rigorous processing of source datasets. This enables boundary conditions to be applied at the domain boundary, and boundary features to be geometrically constrained in the meshing process. It is also necessary to develop a geometric description of regions of the surface geoid, identifying internal interfaces. This is potentially required for the application of:

1. Boundary conditions.
2. Body forcings.
3. Application of model parameterisations.
4. Model coupling.
- 15 5. Initialisation of multiple material phases with differing quantitative properties.
6. Specification of vertical layering.
7. To aid domain decomposition.
8. Accurate calculation of diagnostics.

20 The processing required is exactly that used for geospatial analysis with GIS tools, where regions of a two-dimensional surface are accurately identified. The GIS framework provides a method to approach the accurate identification of regions and their

Integration of GIS into meshing for geophysical models

A. S. Candy et al.

Title Page

Abstract

Introduction

Conclusions

References

Tables

Figures



Back

Close

Full Screen / Esc

Printer-friendly Version

Interactive Discussion



Integration of GIS into meshing for geophysical models

A. S. Candy et al.

Title Page

Abstract

Introduction

Conclusions

References

Tables

Figures



Back

Close

Full Screen / Esc

Printer-friendly Version

Interactive Discussion



interfaces within the computational domain. These can then be used to apply boundary conditions or body forcings to specific areas of the domain, for different coefficients of surface friction for example. This could be used to apply the effect of different land types on inundation flow in a flood model (Gallegos et al., 2009), or for the immersed boundary method to flow over or around under-resolved fine-scale structures, such as man-made sea defences (Viré et al., 2012), or complex networks of coral reefs (Chang et al., 2004). It is also required for the accurate application of parameterisations such as those that model the physics of surface melting from sea ice or ice shelf ocean cavities, for example.

Additionally, identified regions can be used to guide the mesh metric generation for further constraint to ensure an accurate geometric representation of identified features. Further to this, it is possible to direct meshing algorithms to ensure a faithful representation of internal boundaries, including those of the prescribed regions, aligning element faces along these interfaces. This is important to model coupling or the simulation of multiple material phases concurrently, where the position and shape of interfaces transferring information between these must be adequately prescribed.

In the case of ice shelf ocean cavities, for example, there are effectively two bounds on the surface geoid: the coastline, where the ice meets the ocean; and the grounding line, where ice meets bedrock. The union of these defines the fully encompassing surface geoid, but the sub-regions are required to be defined accurately with element faces aligned to those boundaries internal to the domain. This is mitigated to a degree by conservative interpolation methods, such as that of Farrell et al. (2009) developed for arbitrarily unstructured meshes, but there are gains in efficiency and simplifications if the meshes of different regions align exactly at their interface.

Regions can also dictate computational aspects of simulations, such as how the vertical mesh should be constructed (Griffies et al., 2000), with for example, z coordinates or σ layers. They can also guide domain decomposition, when, for example, there is geographic information pertinent to load partitioning. This could occur for regions that are

known to incur a different level of computational expense due to coupling, or specific input data requirements, for example.

GIS tools facilitate the accurate geometric specification of regions and their identification, for multiple and complex forms; and this is the subject of this section.

5.1 Identification and geometric specification of beaches and the fleet lagoon flats

As an example, we develop a geometric description of the beaches and flats in the case study of the Isle of Portland introduced above, in Sect. 4. These regions lie within the surface geoid domain defined by the boundary representation established above, based on the tidal water boundary. Tidal flats, such as the East Fleet highlighted in Fig. 10a, are important ecosystems that often support a large population of wildlife, and are in particular, a vital habitat for migratory shorebirds. There is scientific motivation for an accurate geometric representation of these regions. This includes an improvement of models of tidal incursion into the lagoon with an inhomogeneous treatment of bottom drag, in predictions of future sediment deposit, effects of the dispersion of pollutants, and an accurate calculation of diagnostics, such as depth-integrated flow to infer sediment transport over the flat regions. Identification of these regions also allow for special treatment when wetting-and-drying schemes are applied, or for a specific evaluation of flood risk.

The shape of the flats and beach around the East Fleet region behind Chesil Beach are the focus of Fig. 10a, which contains a portion of the *OS Street View* SY67NW tile. In this case, we do not have a vector representation of the beaches or flats. To generate an accurate boundary representation of the flats and beach edges the *OS Street View* raster is contoured using a GIS raster operation. The contours are then cleaned up in GIS, to remove paths related to text labels for example, which cross the regions in places. The individual paths are then formed into polygons to create distinct regions. In the case of the beaches, the land polygon generated earlier is subtracted from the new polygon containing the beaches to pick out the beaches alone. The result of this

Integration of GIS into meshing for geophysical models

A. S. Candy et al.

Title Page

Abstract

Introduction

Conclusions

References

Tables

Figures



Back

Close

Full Screen / Esc

Printer-friendly Version

Interactive Discussion



Integration of GIS into meshing for geophysical models

A. S. Candy et al.

Title Page

Abstract

Introduction

Conclusions

References

Tables

Figures



Back

Close

Full Screen / Esc

Printer-friendly Version

Interactive Discussion



GIS processing is shown in Fig. 10b, with the flats grouped into a single multi-part polygon shapefile layer and highlighted in yellow and the beaches similarly grouped and shown in red. Using this process we have been able to describe these regions with a great amount of detail, down to very small scales at the accuracy of the source data. This is the boundary representation provided to the meshing algorithm. It is up to the characteristic element length scale metric to determine how well these regions are represented in the discretised domain. It is important to provide a high resolution representation at this stage, and this is competently handled by the GIS framework.

6 Materials: assimilation of source datasets

In the generation of a geometric specification of the external and internal boundaries above, several sources of information were brought in to inform the process. The vector and raster formats used have been designed for geospatial analysis and the GIS tool handles them competently together in a single interface. In the preparation of the data required by the meshing tool, the boundary representation and metric need to be developed so they are mutually consistent. For example, rasters may not be spatially-complete over the required computational domain, or the domain may include regions in the raster that are defined with a different use (e.g. land within an area defined as ocean by the boundary representation, for an ocean simulation). This is typically fixed using *infill* routines to fill in missing values by an interpolation using the solution to a diffusion problem, for example; or using data only where it is available when a functional of multiple datasets is used. This is easier to achieve in a GIS framework, where the individual layers can be inspected in a spatially-consistent environment. This is a prevalent problem in simulation initialisation, where an informed functional assimilation of datasets is required.

This demands an approach similar to the process of *cartographic modelling* (Tomlin, 1990) where multiple thematic layers of an area are created, edited, operated on and analysed. Models for simulation (e.g. flood models following hydrodynamic flow laws)

Integration of GIS into meshing for geophysical models

A. S. Candy et al.

Title Page

Abstract

Introduction

Conclusions

References

Tables

Figures



Back

Close

Full Screen / Esc

Printer-friendly Version

Interactive Discussion



and optimisation (e.g. of land use, transport network planning and data assimilation) can be formed through operations on these map layers. The steps required in generating a suitable dataset for initialisation of a bathymetric height map from multiple sources, and hence map layers, are described in detail in Bailly du Bois (2011), and an approach to automate this suggested.

Algorithms to apply mesh gradation methods (Alauzet, 2010), metric regularisation (as in van Scheltinga et al., 2012 to ensure adequate resolution within the channels of archipelago networks), or shape-optimisation methods to ensure an adequate representation of bathymetric (Gorman et al., 2006) and boundary (Gorman et al., 2007) features based on surface curvature, are examples of a wealth of methods developed to aid metric constraint. These are not accessible through an appropriate common interface, and for geophysical models at least, GIS frameworks are a suitable platform to integrate these tools.

We will now consider metric generation for the example case, that is consistent to the boundary representation, and bring in further datasets, with a large disparity of scales and resolution, and in dataset size.

6.1 Metric generation within a GIS framework

For geophysical models, the metric is one of several required fields defined on a two-dimensional surface. A GIS framework is good stage for these to be developed and prototyped within.

To ensure a good representation of the external boundary representation, it is common to focus the resolution of representation close to these boundaries (Heinzer et al., 2012). This is achieved by a metric based on proximity to the boundary, typically calculated through the solution of a Laplacian diffusion problem. This is available as a GIS tool, commonly provided by the GDAL (Geospatial Data Abstraction Library, 2014) library, and involves the conversion of a vector layer to a raster layer.

In the case under study, to calculate the proximity to the coastline, a multi-part vector layer is formed, with a binary split in identification references, with 0 for the ocean

framework. Within this, it was easy to take an existing tool designed to work on standardised data and GIS layers and develop it further to extend its capabilities for the application under consideration. These developments are now fed back into the community for use by others in similar applications, and potentially many other future works not yet considered.

The metric developed so far ensures an accurate representation of the external boundary representation and other interfaces on the surface geoid. To additionally ensure an accurate representation of the domain in the remaining dimension, locally perpendicular to this surface, the two height fields $b : \Omega \mapsto \mathbb{R}$ and $h : \Omega \mapsto \mathbb{R}$, for the top (height-defined) and bottom (bathymetry-defined) surfaces are considered. To incorporate mesh constraints based on these surfaces, functions acting directly on the two-dimensional raster fields are required, instead of the vector that describes the shape in the other dimensions.

The GEBCO data used to represent bathymetry in the metric generation developed in Fig. 1 is not of high enough resolution in this coastal region. A higher-resolution dataset covering this coastal region is required. A section of the gridded Marine Digimap Coastal Bathymetry (Marine Digimap, 2008) with a 1 arcsecond grid (approximately 30 m cell size) is shown in Fig. 5. This data is in the ArcInfo Grid format (Environmental Systems Research Institute, 2013), and the four tiles NW55000025, NW55000030, NW55050025 and NW55050030 are required to include the region of interest. This covers the region $[-3.0, -2.0] \times [50.0, 51.0]$, for longitude-latitude coordinates (ψ, ϕ) . Distributed as a standard format, the metadata describing this data notes it is stored under the projection WGS 84, about major equatorial radius 6 378 137.0 m and flattening $1/298.257223563$, which the GIS interprets automatically and projects on-the-fly to the common projection selected for the GIS interface. In the process of its preparation for the meshing algorithm, the first step is to combine the four distinct datasets of the tiles into a single raster, which is trivial to achieve in the GIS framework using a raster merge operation, which automatically takes into account metadata on the projection, resolution and location. The resulting raster layer represents the

GMDD

7, 5993–6060, 2014

Integration of GIS into meshing for geophysical models

A. S. Candy et al.

Title Page

Abstract

Introduction

Conclusions

References

Tables

Figures



Back

Close

Full Screen / Esc

Printer-friendly Version

Interactive Discussion



function $b(\mathbf{x}) : \Omega \mapsto \mathbb{R}$, from two-dimensional parameter space Ω to \mathbb{R} , a description of the bathymetry in Ω . To generate a metric of appropriate characteristic edge length sizes, the following functional is developed

$$\mathcal{M}_b(\mathbf{x}) = \max((-b(\mathbf{x}) - 8.0) \times 50.0, 100.0). \quad (2)$$

This scales the bathymetry and also ensures a minimum length scale of 100 m in shallow regions of 0–10 m, to allow the proximity metric to dictate behaviour there. The resulting raster layer represents the functional $\mathcal{M}_b : \Omega \mapsto \mathbb{R}^2 \times \mathbb{R}^2$, from two-dimensional parameter space Ω to a tensor field in $\mathbb{R}^2 \times \mathbb{R}^2$, and is shown in Fig. 12a.

The metric shown in Fig. 12c, is a combination of three raster layers representing \mathcal{M}_b , \mathcal{M}_c and \mathcal{M}_f , combining the metric developed in Eq. (1) with the higher-resolution bathymetry data introduced above, to give the following functional

$$\begin{aligned} \mathcal{M}(\mathbf{x}) &= F(\mathcal{M}_p, \mathcal{M}_b, \mathcal{M}_s), \\ &= \min(\mathcal{M}_p, \mathcal{M}_b, \mathcal{M}_s), \end{aligned} \quad (3)$$

where $\mathcal{M}_s \in \mathbb{R}^2 \times \mathbb{R}^2$ is an isotropic metric representing a constant maximum background element length sizing.

The boundary representation of Figs. 9 and 10b, and domain-complete metric developed in Fig. 12c, together with boundary and region identifications, are sufficient to fully constrain the discretisation of the two-dimensional geoid surface. The constraint information is stored within a QGIS project in standard formats (ESRI shapefile for boundary representation, and GeoTIFF or NetCDF for metric). With the help of GIS tools, including the plugins in the implementation of the approach considered here, this is converted into formats suitable for the meshing algorithm implementation chosen, which here is Gmsh. In this case the boundary representation and identification information is generated and stored using Gmsh syntax (i.e. in a `.geo` file format). The gridded data of the raster layer is converted to a structured field format (Geuzaine and Remacle, 2014, page 54) for Gmsh to read. There is no transformation of the data

Integration of GIS into meshing for geophysical models

A. S. Candy et al.

Title Page	
Abstract	Introduction
Conclusions	References
Tables	Figures
◀	▶
◀	▶
Back	Close
Full Screen / Esc	
Printer-friendly Version	
Interactive Discussion	



in this process, both the input and output data types are stored on regular structured grids, and this process is purely for interoperability, necessary in this case because the tools do not share a common format.

The interface with the meshing algorithms must ensure that description of the boundary representation and metric are such that the meshing process takes place in an appropriate map projection. This is typically the projection used in the simulation code.

In this case, since the horizontal extent is relatively small such that distortion due to the curvature of the Earth is not significant, the geoid surface mesh is generated in a flat two-dimensional plane from a projection in UTM zone 30U.

The result of meshing to these constraints on the two-dimensional surface geoid is shown in Fig. 13. Both large-scale coastline features and the small-scale man-made constructs in the harbour are captured in the boundary. The complex harbour structures seen in Fig. 14 are well-represented and have been accurately established in the mesh using GIS tools under a common projection. The mesh also resolves shallower features such as the Shambles Bank to the east of the southern tip of the isle (marked in Fig. 5). This is the main eastern headland shelf deposit containing bioclastic sand and gravel, due to the main offshore race from Portland (Bastos et al., 2003). An increase in resolution close to the east side of the coast around the isle can be seen in the element edge lengths too of Fig. 13a, as is the long shallow extent of Weymouth beach. These mesh features have been driven by the contribution of bathymetry to the overall edge length metric, shown in Fig. 12, and mirror the features observed in this field.

In the case of multiple scales and resolutions of data required in the construction of the metric, multiple fields are input into the meshing tool for combination at the meshing stage. This is an approach to deal with datasets with a large disparity of scales, a workaround for the limited flexibility of structured data types. This approach is used with the Gmsh meshing tool in the generation of the Isle of Portland region nested in the North Sea domain considered later, the result of which is presented in Fig. 16.

Integration of GIS into meshing for geophysical models

A. S. Candy et al.

Title Page

Abstract

Introduction

Conclusions

References

Tables

Figures



Back

Close

Full Screen / Esc

Printer-friendly Version

Interactive Discussion



Integration of GIS into meshing for geophysical models

A. S. Candy et al.

Title Page

Abstract

Introduction

Conclusions

References

Tables

Figures

⏪

⏩

◀

▶

Back

Close

Full Screen / Esc

Printer-friendly Version

Interactive Discussion



The mesh of the region centred around the East Flats is shown in Fig. 15, together with the boundary representation generated with GIS. Figure 15a shows the mesh that corresponds to the metric Eq. (3) with $\alpha = 0.4$ and $\beta = 0.8$, with $\gamma = \frac{1}{2}$, such that proximity to the internal boundary of the flats is given half the weighting as the proximity to the coastline. This gives a very accurate representation of the regions and their boundaries, that closely follows the provided boundary representation. If this fidelity of representation of these interfaces is relaxed by choosing $\beta = 6.0$, such that $\gamma = \frac{1}{15}$ as shown in Fig. 15b, the regions are still well-represented, but without the concentration of mesh nodes about the region interfaces. This is a compromise that can be easily managed and prototyped using a GIS framework as a preprocessing stage for data preparation for meshing algorithms.

6.2 Multi-scale discretisation

Integration of mesh initialisation into GIS makes it possible to easily interpret and combine datasets, and further simulation efforts over a range of scales. For example, it is now an easy progression to combine the two cases studied above, the large-scale North Sea region and the smaller coastal scale region centred around the Isle of Portland. With a large scale model developed, the results can be used to initially force the smaller coastal model, and with the GIS framework, the domains can be combined. The shapefiles detailing the boundary representation are simply merged within GIS, with possible corrections informed by map information in the same interface. The raster fields are also merged to define a metric for the entire domain, including fine-scale features in the small region of interest. As noted above, due to the limitations of the structured raster fields, it may be more efficient to supply multiple metric fields to the meshing algorithm. We consider this combination of domains over scales now.

The metric for the North Sea case presented in Fig. 3c, is generated from a function of bathymetry \overline{M}_b (shown in a), and of proximity to coastline \overline{M}_c (shown in b), together with an isotropic metric representing a constant maximum background element length

sizing $\overline{\mathcal{M}}_s$. In a similar manner to the metric for the Portland Bill region \mathcal{M} , these are combined according to the functional

$$\begin{aligned}\overline{\mathcal{M}}(\mathbf{x}) &= F(\overline{\mathcal{M}}_b, \overline{\mathcal{M}}_c, \overline{\mathcal{M}}_s), \\ &= \min(\overline{\mathcal{M}}_b, \overline{\mathcal{M}}_c, \overline{\mathcal{M}}_s),\end{aligned}\quad (4)$$

where the bathymetry metric is developed according to

$$\overline{\mathcal{M}}_b(\mathbf{x}) = 5.0 \times 10^3 \times 10^{\left(\frac{\delta-10.0}{200.0-10.0}\right)^3}.\quad (5)$$

Here a limited bathymetry function is defined by

$$\delta(\mathbf{x}) = \max(\min(\max(-\overline{b}(\mathbf{x}), 0.0), 200.0), 10.0),$$

for the bathymetry function $\overline{b}(\mathbf{x})$ of Fig. 2a, which focuses on the range of depths $\delta \in [10.0, 200.0]$. This gives a metric field with characteristic length scales ranging from 5 km to 50 km. The form of the metric functional applied here has been chosen to identify shallow bathymetric features in this example case, with an appropriate gradation of mesh size into deeper regions. It demonstrates that relatively complex functional forms can be prototyped and developed in a straightforward manner using GIS raster layers and tools.

The coastline proximity metric is generated from the proximity field $\overline{\rho}(\mathbf{x})$, shown in Fig. 2b and follows

$$\overline{\mathcal{M}}_c(\mathbf{x}) = (10^5 - 2.5 \times 10^3) \frac{\overline{\rho}(\mathbf{x}) - 10^4}{2.0 \times 10^5 - 10^4} + 2.5 \times 10^3,\quad (6)$$

to give a range of characteristic length scales over 2.5 km to 100 km for $\overline{\rho}(\mathbf{x})$ from 10 km to 200 km. The combined metric field $\overline{\mathcal{M}}$ for the North Sea has been developed in GIS together with its consistent boundary representation.

Integration of GIS into meshing for geophysical models

A. S. Candy et al.

Title Page

Abstract

Introduction

Conclusions

References

Tables

Figures



Back

Close

Full Screen / Esc

Printer-friendly Version

Interactive Discussion



The nesting of the Isle of Portland region within this North Sea domain is easy to achieve within a GIS framework, which handles datasets of differing scales and resolution together competently. The fine scale boundary representation of Figs. 7, 9 and 10b is joined to the larger scale boundary representation on the Northsea region of Fig. 1.

5 The metrics are combined, under a functional F , to give

$$\begin{aligned}\overline{\mathcal{M}}(\mathbf{x}) &= F(\mathcal{M}_b, \mathcal{M}_c, \overline{\mathcal{M}}_b, \overline{\mathcal{M}}_c, \overline{\mathcal{M}}_s), \\ &= \min(\mathcal{M}_b, \mathcal{M}_c, \overline{\mathcal{M}}_b, \overline{\mathcal{M}}_c, \overline{\mathcal{M}}_s),\end{aligned}\quad (7)$$

10 taking into account the bathymetry and coastline proximity of the two domains considered.

It is also worthy of note that the above considers a scalar-valued metric, where $\mathcal{M} : \mathbb{R}^2 \mapsto \mathbb{R}$, for a given projection. Anisotropic metrics, where $\mathcal{M} : \mathbb{R}^2 \mapsto \mathbb{R}^2 \times \mathbb{R}^2$, could be achieved in GIS with two orthogonal component layers, or a Hessian calculation of a scalar layer.

15 6.3 Full mesh generation

Much of the challenge in the generation of meshes for geophysical models is in the development of a mesh of the surface geoid. This is all that is required for shallow water modelling for example. A full three-dimensional mesh can be generated by an advancing-front algorithm to extrude top and bottom bounds from the meshed surface geoid. It is possible to generate these surface bounds within GIS, as raster layers with coverage over the boundary representation. How the resolution varies vertically can be described by a metric in full three-dimensional space, or simplified as a function of height (for z coordinates) or as a function of proportional height (σ -layers), and divided spatially by regions over the geoid surface.

Integration of GIS into meshing for geophysical models

A. S. Candy et al.

Title Page	
Abstract	Introduction
Conclusions	References
Tables	Figures
⏪	⏩
◀	▶
Back	Close
Full Screen / Esc	
Printer-friendly Version	
Interactive Discussion	



7 Conclusions and perspectives

This paper successfully demonstrates the integration of technologies, bringing GIS, meshing and numerical simulation models together, to develop an approach to accurate, rigorous and efficient domain initialisation for geophysical models with complex boundaries.

Model initialisation is becoming more of a challenge as the complexity of simulation codes increases. The problem of specifying model options and parameters in multi-physics models has been tackled through self-validating parameter-comprehensive tools such as Spud (Ham et al., 2009). Similarly, another aspect of model initialisation, domain discretisation, is becoming more of a challenge as models simulate over a larger range of scales in more realistic geometries. The problem of assimilating all of the input data and defining an accurate description of the parameter space to fully constrain the domain discretisation presents a serious cost in model setup time, and a significant barrier to the development of more complex domains generated consistently and error-free from multiple sources of data.

The presented approach is a significant departure from existing practice in geoscientific models. Through engaging with established GIS tools and adopting standardised data formats and interfaces, we have developed a practical process for the rigorous generation of meshes for geophysical models. The approach taken builds on standard tools, with a hierarchy of automation such that operations can be broken down to finer low-level manipulations. For complex large vector paths, or high resolution raster data, efficiency and memory demands mean it is sometimes necessary to identify the process required and apply the operation outside of the GIS framework, potentially in a parallel High Performance Computing setting. This is possible when standardised libraries and methods are employed and such a hierarchy of automation exists. This structure also allows for progressively lower-level operations to be made for finer edits and in the example case here, made it possible to easily adjust the boundary around Portland Harbour to open up Ferry Bridge using another contour and exposed

GMDD

7, 5993–6060, 2014

Integration of GIS into meshing for geophysical models

A. S. Candy et al.

Title Page

Abstract

Introduction

Conclusions

References

Tables

Figures



Back

Close

Full Screen / Esc

Printer-friendly Version

Interactive Discussion



discipline-independent infrastructure that makes the data accessible for analysis and visualization are vital to advancing insight into our world.

Appendix A: Code availability, distribution and licensing

The *QGIS-Meshing plugins* developed to enable this study are available from the Applied Modelling and Computation Group at Imperial College London, and further information can be found at <http://www.gismeshing.org>, with the source code hosted in the repository located at <http://github.com/gismeshing/QGIS-Meshing>. Supplementary data associated with this article can be found there also, which includes a manual to the *QGIS-Meshing plugins* and details of obtaining them. The plugins are routinely verified by a build engine (Farrell et al., 2011) and its status is available at the pages above, together with source code, verification tests and examples.

All components of the package are free software, being released under the GNU Lesser General Public License version 2.1. This combination of licenses ensures that the plugins can legally be used with models which employ a wide range of licensing schemes, both free and proprietary. Full details of the licenses, including the (compatible) copyright notices of some third party routines included in the package, are included in COPYING in the source distribution.

Acknowledgements. The authors wish to acknowledge support from the U.K. Natural Environment Research Council (NERC, grant NE/G018391/1) and the Engineering and Physical Sciences Research Council (grant EP/I00405X/1). Additional support was provided by Imperial College London through its short internship UROP studentships, specifically from the Department of Earth Science and Engineering and the Royal School of Mines Association, and NERC from its Research Experience Placement grants. The authors would like to thank Shaun Lee, Elliot Lynch, Mihai Jiplea and Varun Verma for their help in the development and testing of the code used to implement the approach introduced here.

GMDD

7, 5993–6060, 2014

Integration of GIS into meshing for geophysical models

A. S. Candy et al.

Title Page

Abstract

Introduction

Conclusions

References

Tables

Figures



Back

Close

Full Screen / Esc

Printer-friendly Version

Interactive Discussion



References

- Adcroft, A. and Marshall, D.: How slippery are piecewise-constant coastlines in numerical ocean models?, *Tellus A*, 50, 95–108, doi:10.1034/j.1600-0870.1998.00007.x, 1998. 5995
- Adcroft, A., Hill, C., and Marshall, J.: Representation of topography by shaved cells in a height coordinate ocean model, *Mon. Weather Rev.*, 125, 2293–2315, 1997. 5995
- Ahrens, J., Law, C., Schroeder, W., Martin, K., and Papka, M.: A parallel approach for efficiently visualizing extremely large, time-varying datasets, Tech. Rep.# LAUR-00-1620, Los Alamos National Laboratory, 2000. 6030
- Alauzet, F.: Size gradation control of anisotropic meshes, *Finite Elem. Anal. Des.*, 46, 181–202, doi:10.1016/j.finel.2009.06.028, 2010. 6020
- Antoniou, B. and Tsoulos, L.: The potential of XML encoding in geomatics converting raster images to XML and SVG, *Comput. Geosci.*, 32, 184–194, doi:10.1016/j.cageo.2005.06.004, 2006. 6003, 6004
- Arya, S., Mount, D., Netanyahu, N., Silverman, R., and Wu, A.: An optimal algorithm for approximate nearest neighbor searching fixed dimensions, *J. ACM*, 45, 891–923, 1998. 6005
- Bailly du Bois, P.: Automatic calculation of bathymetry for coastal hydrodynamic models, *Comput. Geosci.*, 37, 1303–1310, doi:10.1016/j.cageo.2010.11.018, 2011. 6020
- Bastos, A., Collins, M., and Kenyon, N.: Water and sediment movement around a coastal headland: Portland Bill, southern UK, *Ocean Dynam.*, 53, 309–321, 2003. 6012, 6024
- Bernard, B., Madec, G., Penduff, T., Molines, J.-M., Treguier, A.-M., Sommer, J., Beckmann, A., Biastoch, A., Böning, C., Dengg, J., Derval, C., Durand, E., Gulev, S., Remy, E., Talandier, C., Theetten, S., Maltrud, M., McClean, J., and Cuevas, B.: Impact of partial steps and momentum advection schemes in a global ocean circulation model at eddy-permitting resolution, *Ocean Dynam.*, 56, 543–567, doi:10.1007/s10236-006-0082-1, 2006. 5995
- Bilgili, A., Smith, K. W., and Lynch, D. R.: BatTri: a two-dimensional bathymetry-based unstructured triangular grid generator for finite element circulation modeling, *Comput. Geosci.*, 32, 632–642, 2006. 5997
- Blain, C. A., Linzell, R. S., and Massey, T. C.: MeshGUI: a mesh generation and editing toolset for the ADCIRC model, Tech. rep., DTIC Document, 2008. 5997
- Blain, C. A., Linzell, R. S., Weidemann, A. D., and Lyon, P. E.: A tool for rapid configuration of a river model, in: *OCEANS 2009, MTS/IEEE Biloxi-Marine Technology for Our Future: Global and Local Challenges*, IEEE, 1–10, 2009. 5997

Integration of GIS into meshing for geophysical models

A. S. Candy et al.

Title Page

Abstract

Introduction

Conclusions

References

Tables

Figures



Back

Close

Full Screen / Esc

Printer-friendly Version

Interactive Discussion



Integration of GIS into meshing for geophysical models

A. S. Candy et al.

Title Page

Abstract

Introduction

Conclusions

References

Tables

Figures



Back

Close

Full Screen / Esc

Printer-friendly Version

Interactive Discussion



- Blunden, L. and Bahaj, A.: Initial evaluation of tidal stream energy resources at Portland Bill, UK, *Renew. Energ.*, 31, 121–132, 2006. 6012
- Bray, M.: Coastal sediment supply and transport, in: *The Coastal Landforms of West Dorset*, edited by: Allison, R., The Geologists' Association, 1992. 6013
- 5 Cartographic Projections Library: PROJ.4 – Cartographic Projections Library, available at: <http://trac.osgeo.org/proj> (last access: 20 May 2014), 2014. 6011
- Casarotti, E., Stupazzini, M., Lee, S., Komatitsch, D., Piersanti, A., and Tromp, J.: GEOCUBIT, an HPC parallel mesher for Spectral-Element Method seismic wave simulation, 70th EAGE Conference & Exhibition-Workshops and Fieldtrips, 2008. 5996
- 10 CASCADOSS: Development of a trans-national cascade programme on Open Source GIS&RS Software for environmental applications. Funded under the European Commission Sixth Framework Programme for the identification of new methods of promoting and encouraging trans-national technology., available at: <http://cascadoss.gridw.pl/en/> (last access: 20 May 2014), 2009. 5999, 6011
- 15 CESM: Community Earth System Model, available at: <http://www2.cesm.ucar.edu> (last access: 20 May 2014), 2014. 6008
- Chang, S., Iaccarino, G., Elkins, C., Eaton, J., and Monismith, S.: A Computational and Experimental Investigation of Flow Inside Branched Coral Colony, *Center for Turbulence Research Ann. Res. Briefs, NASA Ames/Stanford University*, 45–54, 2004. 6017
- 20 Chen, C., Liu, H., and Beardsley, R. C.: An unstructured grid, finite-volume, three-dimensional, primitive equations ocean model: application to coastal ocean and estuaries, *J. Atmos. Ocean. Tech.*, 20, 159–186, 2003. 5995
- Chen, D., Shams, S., Carmona-Moreno, C., and Leone, A.: Assessment of open source GIS software for water resources management in developing countries, *Journal of Hydro-environment Research*, 4, 253–264, doi:10.1016/j.jher.2010.04.017, 2010. 5999, 6011
- 25 Comer, D.: Ubiquitous B-Tree, *ACM Comput. Surv.*, 11, 121–137, doi:10.1145/356770.356776, 1979. 6010
- COMSOL, 2014: COMSOL Multiphysics, available at: <http://www.comsol.com> (last access: 20 May 2014), 2014. 5996
- 30 Conroy, C. J., Kubatko, E. J., and West, D. W.: ADMESH: an advanced, automatic unstructured mesh generator for shallow water models, *Ocean Dynam.*, 62, 1503–1517, 2012. 6006
- Cubit Development Team and Jankovich, S. R.: CUBIT Mesh Generation Environment Volume 1: Users Manual, 2014. 5996

Integration of GIS into meshing for geophysical models

A. S. Candy et al.

Title Page

Abstract

Introduction

Conclusions

References

Tables

Figures



Back

Close

Full Screen / Esc

Printer-friendly Version

Interactive Discussion



- Danilov, S., Kivman, G., and Schröter, J.: A finite-element ocean model: principles and evaluation, *Ocean Model.*, 6, 125–150, doi:10.1016/S1463-5003(02)00063-X, 2004. 5995
- de Brye, B.: Multiscale Finite-Element Modelling of River-Sea Continua, Ph.D. thesis, Institut de Mécanique, Matériaux et Génie Civil, Université catholique de Louvain, 2011. 6003
- 5 Defoe, D.: The Storm, a Collection of the most Remarkable Casualties and Disasters which Happen'd in the Late Dreadful Tempest, both by Sea and Land, George Sawbridge, London, 1703. 6013
- DHI Group: MIKE, available at: <http://www.mikebydhi.com> (last access: 20 May 2014), 2014. 5995, 5997
- 10 Dietrich, J., Kolar, R., and Dresback, K.: Mass residuals as a criterion for mesh refinement in continuous Galerkin shallow water models, *J. Hydraul. Eng.*, 134, 520–532, 2008. 6006
- Douglas, D. H. and Peucker, T. K.: Algorithms for the reduction of the number of points required to represent a digitized line or its caricature, *Cartographica: The International Journal for Geographic Information and Geovisualization*, 10, 112–122, 1973. 6006, 6008
- 15 Dunfey, R. I., Gittings, B. M., and Batcheller, J. K.: Towards an open architecture for vector GIS, *Comput. Geosci.*, 32, 1720–1732, doi:10.1016/j.cageo.2006.04.004, 2006. 6003
- Eaton, B., Gregory, J. M., Drach, B., Taylor, K., Hankin, S., Caron, J., and Signell, R.: NetCDF Climate and Forecast (CF) Metadata Conventions, Version 1.1, available at: <http://cf-pcmdi.llnl.gov/documents/cf-conventions/1.1/cf-conventions.pdf> (last access: 20 May 2014), 2008. 5996, 6010
- 20 Environmental Systems Research Institute: ESRI ArcInfo Grid format, available at: <http://help.arcgis.com/en/arcgisdesktop/10.0/help/009t/009t0000000w000000.htm> (last access: 20 May 2014), 2013. 6022
- ERSI ArcGIS Platform: ArcGIS, available at: <http://www.arcgis.com> (last access: 20 May 2014), 2014. 5997, 6006, 6030
- 25 ESRI: Environmental Systems Research Institute (ESRI) Shapefile Technical Description: An ESRI White Paper, 1998. 6003, 6010
- Farrell, P., Piggott, M., Pain, C., Gorman, G., and Wilson, C.: Conservative interpolation between unstructured meshes via supermesh construction, *Comput. Method. Appl. M.*, 198, 2632–2642, doi:10.1016/j.cma.2009.03.004, 2009. 6017
- 30 Farrell, P. E., Piggott, M. D., Gorman, G. J., Ham, D. A., Wilson, C. R., and Bond, T. M.: Automated continuous verification for numerical simulation, *Geosci. Model Dev.*, 4, 435–449, doi:10.5194/gmd-4-435-2011, 2011. 5995, 6031

Integration of GIS into meshing for geophysical models

A. S. Candy et al.

Title Page

Abstract

Introduction

Conclusions

References

Tables

Figures



Back

Close

Full Screen / Esc

Printer-friendly Version

Interactive Discussion



- Galland, J.-C., Goutal, N., and Hervouet, J.-M.: TELEMAC: a new numerical model for solving shallow water equations, *Adv. Water Resour.*, 14, 138–148, doi:10.1016/0309-1708(91)90006-A, 1991. 5995, 5997, 6011, 6012
- Gallegos, H. A., Schubert, J. E., and Sanders, B. F.: Two-dimensional, high-resolution modeling of urban dam-break flooding: a case study of Baldwin Hills, California, *Adv. Water Resour.*, 32, 1323–1335, doi:10.1016/j.advwatres.2009.05.008, 2009. 6017
- Geographic Resources Analysis Support System: Geographic Resources Analysis Support System (GRASS), available at: <http://grass.osgeo.org> (last access: 20 May 2014), 2014. 6011
- Geospatial Data Abstraction Library: Geospatial Data Abstraction Library, available at: <http://www.gdal.org> (last access: 20 May 2014), 2014. 6011, 6020
- Geuzaine, C. and Remacle, J.-F.: Gmsh: a 3-D finite element mesh generator with built-in pre- and post-processing facilities, *Int. J. Numer. Meth. Eng.*, 79, 1309–1331, doi:10.1002/nme.2579, 2009. 5996, 6002
- Geuzaine, C. and Remacle, J.-F.: Gmsh reference manual, version 2.8, Gmsh: a Finite Element Mesh Generator with Built-in Pre-and Post-Processing Facilities, 2014. 6023
- Gorman, G., Piggott, M., Pain, C., de Oliveira, C., Umpleby, A., and Goddard, A.: Optimisation based bathymetry approximation through constrained unstructured mesh adaptivity, *Ocean Model.*, 12, 436–452, doi:10.1016/j.ocemod.2005.09.004, 2006. 5998, 6002, 6006, 6020, 6029
- Gorman, G., Piggott, M., and Pain, C.: Shoreline approximation for unstructured mesh generation, *Comput. Geosci.*, 33, 666–677, doi:10.1016/j.cageo.2006.09.007, 2007. 6002, 6006, 6010, 6020, 6029
- Gorman, G., Piggott, M., Wells, M., Pain, C., and Allison, P.: A systematic approach to unstructured mesh generation for ocean modelling using GMT and Terreno, *Comput. Geosci.*, 34, 1721–1731, doi:10.1016/j.cageo.2007.06.014, 2008. 6003
- Gourgue, O., Comblen, R., Lambrechts, J., Kärnä, T., Legat, V., and Deleersnijder, E.: A flux-limiting wetting-drying method for finite-element shallow-water models, with application to the Scheldt Estuary, *Adv. Water Resour.*, 32, 1726–1739, 2009. 6003
- Gourgue, O., Baeyens, W., Chen, M., de Brauwere, A., de Brye, B., Deleersnijder, E., Elskens, M., and Legat, V.: A depth-averaged two-dimensional sediment transport model for environmental studies in the Scheldt Estuary and tidal river network, *J. Marine Syst.*, 128, 27–39, doi:10.1016/j.jmarsys.2013.03.014, 2013. 5996

Integration of GIS into meshing for geophysical models

A. S. Candy et al.

Title Page

Abstract

Introduction

Conclusions

References

Tables

Figures



Back

Close

Full Screen / Esc

Printer-friendly Version

Interactive Discussion



- Gregory, J. M.: The CF Metadata Standard, available at: http://cf-pcmdi.llnl.gov/documents/other/cf_overview_article.pdf (last access: 20 May 2014), 2003a. 6009
- Gregory, J. M.: The CF Metadata Standard, CLIVAR Exchanges, 8, 4, available at: http://www.clivar.org/publications/exchanges/ex28/pdf/s28_gregory.pdf (last access: 20 May 2014), 2003b. 5996, 6010
- Griffies, S. M., Böning, C., Bryan, F. O., Chassignet, E. P., Gerdes, R., Hasumi, H., Hirst, A., Treguier, A.-M., and Webb, D.: Developments in ocean climate modelling, *Ocean Model.*, 2, 123–192, doi:10.1016/S1463-5003(00)00014-7, 2000. 5995, 6017
- Griffies, S. M., Gnanadesikan, A., Dixon, K. W., Dunne, J. P., Gerdes, R., Harrison, M. J., Rosati, A., Russell, J. L., Samuels, B. L., Spelman, M. J., Winton, M., and Zhang, R.: Formulation of an ocean model for global climate simulations, *Ocean Sci.*, 1, 45–79, doi:10.5194/os-1-45-2005, 2005. 5994
- Griffies, S. M., Biastoch, A., Böning, C., Bryan, F., Danabasoglu, G., Chassignet, E. P., England, M. H., Gerdes, R., Haak, H., Hallberg, R. W., Hazeleger, W., Jungclaus, J., Large, W. G., Madec, G., Pirani, A., Samuels, B. L., Scheinert, M., Gupta, A. S., Severijns, C. A., Simmons, H. L., Treguier, A. M., Winton, M., Yeager, S., and Yin, J.: Coordinated Ocean-ice Reference Experiments (COREs), *Ocean Model.*, 26, 1–46, doi:10.1016/j.ocemod.2008.08.007, 2009. 5996
- Ham, D. A., Farrell, P. E., Gorman, G. J., Maddison, J. R., Wilson, C. R., Kramer, S. C., Ship-ton, J., Collins, G. S., Cotter, C. J., and Piggott, M. D.: Spud 1.0: generalising and automating the user interfaces of scientific computer models, *Geosci. Model Dev.*, 2, 33–42, doi:10.5194/gmd-2-33-2009, 2009. 5995, 6028
- Hastings, S., Kurc, T., Langella, S., Catalyurek, U., Pan, T., and Saltz, J.: Image processing for the grid: A toolkit for building grid-enabled image processing applications, in: *Cluster Computing and the Grid*, 2003. Proceedings. CCGrid 2003. 3rd IEEE/ACM International Symposium on, IEEE, 36–43, 2003. 6030
- HDF5: HDF5, Hierarchical Data Format, available at: <http://www.hdfgroup.org/HDF5> (last access: 20 May 2014), 2014. 6010
- Heinzer, T. J., Williams, M. D., Dogrul, E. C., Kadir, T. N., Brush, C. F., and Chung, F. I.: Implementation of a feature-constraint mesh generation algorithm within a GIS, *Comput. Geosci.*, 49, 46–52, 2012. 6006, 6020

Integration of GIS into meshing for geophysical models

A. S. Candy et al.

Title Page

Abstract

Introduction

Conclusions

References

Tables

Figures



Back

Close

Full Screen / Esc

Printer-friendly Version

Interactive Discussion



- Humbert, A., Kleiner, T., Mohrholz, C.-O., Oelke, C., Greve, R., and Lange, M. A.: A comparative modeling study of the Brunt Ice Shelf/Stancomb-Wills Ice Tongue system, East Antarctica, *J. Glaciol.*, 55, 53–65, doi:10.3189/002214309788608949, 2009. 5996
- Kärnä, T., de Brye, B., Gourgue, O., Lambrechts, J., Comblen, R., Legat, V., and Deleersnijder, E.: A fully implicit wetting-drying method for DG-FEM shallow water models, with an application to the Scheldt Estuary, *Comput. Method. Appl. M.*, 200, 509–524, doi:10.1016/j.cma.2010.07.001, 2011. 6003
- Kramer, S., Cotter, C., and Pain, C.: Solving the Poisson equation on small aspect ratio domains using unstructured meshes, *Ocean Model.*, 35, 253–263, doi:10.1016/j.ocemod.2010.08.001, 2010. 6000
- Lambrechts, J. and Seny, B.: GMSH Workshop: Ocean, Workshop2 (Ocean meshing), 15 September, available at: <https://geuz.org/trac/gmsh/attachment/wiki/FirstGmshWorkshop/WORK2.pdf>, 2011. 6003
- Lambrechts, J., Comblen, R., Legat, V., Geuzaine, C., and Remacle, J.-F.: Multiscale mesh generation on the sphere, *Ocean Dynam.*, 58, 461–473, doi:10.1007/s10236-008-0148-3, 2008. 5996, 6002, 6010
- Le Pard, G.: The Great Storm of 1824, in: *Proceedings of Dorset Natural History and Archaeological Society*, 23–36, 1999. 6013
- Legg, S. and Adcroft, A.: Internal wave breaking at concave and convex continental slopes, *J. Phys. Oceanogr.*, 33, 2224–2246, 2003. 5995
- Legrand, S., Deleersnijder, E., Delhez, E., and Legat, V.: Unstructured, anisotropic mesh generation for the Northwestern European continental shelf, the continental slope and the neighbouring ocean, *Cont. Shelf Res.*, 27, 1344–1356, 2007. 6002
- Li, Q., Ito, K., Wu, Z., Lowry, C. S., and Loheide II, S. P.: COMSOL multiphysics: a novel approach to ground water modeling, *Ground Water*, 47, 480–487, doi:10.1111/j.1745-6584.2009.00584.x, 2009. 5996
- Maddison, J. R., Marshall, D., Pain, C. C., and Piggott, M. D.: Accurate representation of geostrophic and hydrostatic balance in unstructured mesh finite element ocean modelling, *Ocean Model.*, 39, 248–261, doi:10.1016/j.ocemod.2011.04.009, 2011. 6000
- Marine Digimap: Hydrospatial Bathymetry [Raster geospatial data], Updated April 2008, Sea-
Zone Solutions Ltd., UK, Using EDINA Marine Digimap Service, available at: <http://edina.ac.uk/digimap> (last access: 13 November 2013), 2008. 6022, 6047

Integration of GIS into meshing for geophysical models

A. S. Candy et al.

Title Page

Abstract

Introduction

Conclusions

References

Tables

Figures



Back

Close

Full Screen / Esc

Printer-friendly Version

Interactive Discussion



Mazzolari, A., Araújo, M. A. V. C., and Trigo-Teixeira, A.: Improved Advancing Front Mesh Algorithm with Pseudoislands as Internal Fronts, *J. Waterw. Port C.-ASCE*, 140, 1943–5460, 2014. 6002

McKinney, D. C. and Cai, X.: Linking GIS and water resources management models: an object-oriented method, *Environ. Modell. Softw.*, 17, 413–425, doi:10.1016/S1364-8152(02)00015-4, 2002. 6005

Merwade, V., Cook, A., and Coonrod, J.: GIS techniques for creating river terrain models for hydrodynamic modeling and flood inundation mapping, *Environ. Modell. Softw.*, 23, 1300–1311, 2008. 6005

Met Office: The Recent Storms and Floods in the UK, February 2014, available at: http://www.metoffice.gov.uk/media/pdf/1/2/Recent_Storms_Briefing_Final_SLR_20140211.pdf (last access: 20 May 2014), 2014. 6013

Murta, A.: GPC – General Polygon Clipper library, available at: <http://www.cs.man.ac.uk/~toby/gpc> (last access: 20 May 2014), 2014. 6000

Neteler, M., Bowman, M. H., Landa, M., and Metz, M.: GRASS GIS: a multi-purpose open source GIS, *Environ. Modell. Softw.*, 31, 124–130, doi:10.1016/j.envsoft.2011.11.014, 2012. 6011

ODI: Open Data Certificate, available at: <https://certificates.theodi.org> (last access: 20 May 2014), 2014. 6014

OGC: Open Geospatial Consortium, available at: <http://www.opengeospatial.org> (last access: 20 May 2014), 2014. 6004, 6010

OS OpenData: Ordnance Survey OpenData, available at: <https://www.ordnancesurvey.co.uk/opendatadownload> (last access: 1 June 2013), 2013. 6013

Pacanowski, R. C. and Gnanadesikan, A.: Transient response in a z-level ocean model that resolves topography with partial cells, *Mon. Weather Rev.*, 126, 3248–3270, 1998. 5995

Pain, C., Piggott, M., Goddard, A., Fang, F., Gorman, G., Marshall, D., Eaton, M., Power, P., and de Oliveira, C.: Three-dimensional unstructured mesh ocean modelling, *Ocean Model.*, 10, 5–33, doi:10.1016/j.ocemod.2004.07.005, 2005. 5995, 5998, 6002

Piggott, M., Pain, C., Gorman, G., Power, P., and Goddard, A.: h, r, and hr adaptivity with applications in numerical ocean modelling, *Ocean Model.*, 10, 95–113, doi:10.1016/j.ocemod.2004.07.007, 2005. 5998

Piggott, M. D., Gorman, G. J., Pain, C. C., Allison, P. A., Candy, A. S., Martin, B. T., and Wells, M. R.: A new computational framework for multi-scale ocean modelling

Integration of GIS into meshing for geophysical models

A. S. Candy et al.

Title Page

Abstract

Introduction

Conclusions

References

Tables

Figures



Back

Close

Full Screen / Esc

Printer-friendly Version

Interactive Discussion



- based on adapting unstructured meshes, *Int. J. Numer. Meth. Fl.*, 56, 1003–1015, doi:10.1002/flid.1663, 2008. 6002, 6011
- Portland Port: <http://www.portland-port.co.uk> (last access: 20 May 2014), 2014. 6056
- PyQGIS: PyQGIS Developer Cookbook, available at: <http://www.qgis.org/pyqgis-cookbook> (last access: 20 May 2014), 2014. 6010
- Python Software Foundation: Python Programming Language – Official Website, available at: www.python.org (last access: 20 May 2014), 2011. 6011
- Quantum GIS Development Team: Quantum GIS Geographic Information System, Open Source Geospatial Foundation, available at: <http://qgis.osgeo.org> (last access: 20 May 2014), 2012. 6010
- Rew, R., Davis, G., Emmerson, S., Davies, H., Hartnett, E., Heimbigner, D., and Fisher, W.: Network Common Data Form (NetCDF), available at: <http://www.unidata.ucar.edu/netcdf> (last access: 20 May 2014), 2014. 6009, 6011
- Ritter, N. and Ruth, M.: The GeoTiff data interchange standard for raster geographic images, *Int. J. Remote Sens.*, 18, 1637–1647, doi:10.1080/014311697218340, 1997. 6010
- Shen, Z., Luo, J., Zhou, C., Cai, S., Zheng, J., Chen, Q., Ming, D., and Sun, Q.: Architecture design of grid GIS and its applications on image processing based on LAN, *Inform. Sciences*, 166, 1–17, doi:10.1016/j.ins.2003.10.004, 2004. 6030
- Sherman, G.: Desktop GIS: Mapping the Planet with Open Source Tools, Pragmatic Bookshelf, 2008. 6010
- Shewchuk, J. R.: Delaunay refinement algorithms for triangular mesh generation, *Comput. Geom.-Theor. Appl.*, 22, 21–74, 2002. 6006
- Sidorenko, D., Wang, Q., Danilov, S., and Schröter, J.: FESOM under coordinated ocean-ice reference experiment forcing, *Ocean Dynam.*, 61, 881–890, doi:10.1007/s10236-011-0406-7, 2011. 5995, 6002
- Simanjuntak, M. A., Imberger, J., and Nakayama, K.: Effect of stair-step and piecewise linear topography on internal wave propagation in a geophysical flow model, *J. Geophys. Res.-Oceans*, 114, doi:10.1029/2008JC005051, 2009. 5995
- Steiniger, S. and Bocher, E.: An overview on current free and open source desktop GIS developments, *Int. J. Geogr. Inf. Sci.*, 23, 1345–1370, 2009. 5999
- Steiniger, S. and Hunter, A. J.: The 2012 free and open source GIS software map – A guide to facilitate research, development, and adoption, *Comput. Environ. Urban*, 39, 136–150, doi:10.1016/j.compenurbsys.2012.10.003, 2013. 6011

Integration of GIS into meshing for geophysical models

A. S. Candy et al.

Title Page

Abstract

Introduction

Conclusions

References

Tables

Figures



Back

Close

Full Screen / Esc

Printer-friendly Version

Interactive Discussion



- Taylor, K. E., Stouffer, R. J., and Meehl, G. A.: An overview of cmip5 and the experiment design, *B. Am. Meteorol. Soc.*, 93, 485–498, doi:10.1175/BAMS-D-11-00094.1, 2012. 6008
- Terreno Project: A toolkit for 2d and 3d bathymetric mesh generation via anisotropic adaptive mesh methods, available at: <http://www3.imperial.ac.uk/earthscienceandengineering/research/amcg/terreno>, available at: <http://sourceforge.net/projects/terreno/> (last access: 20 May 2014), 2013. 6010
- The CGAL Project: CGAL User and Reference Manual, CGAL Editorial Board, 4.3 edn., available at: <http://doc.cgal.org/4.3/Manual/packages.html> (last access: 20 May 2014), 2013. 6000, 6011
- The Guardian: Sirens heralded storm that changed the shape of Chesil beach, 7 January 2014, available at: <http://www.theguardian.com/uk-news/2014/jan/07/uk-floods-chesil-beach-sirens> (last access: 20 May 2014), 2014. 6013
- Thomas, C. J., Lambrechts, J., Wolanski, E., Traag, V. A., Blondel, V. D., Deleersnijder, E., and Hanert, E.: Numerical modelling and graph theory tools to study ecological connectivity in the Great Barrier Reef, *Ecol. Model.*, 272, 160–174, doi:10.1016/j.ecolmodel.2013.10.002, 2014. 5996
- Tomlin, C. D.: *Geographic Information Systems and Cartographic Modelling*, Prentice Hall, New Jersey, 1990. 6019
- UKHO: United Kingdom Hydrographic Office, Admiralty Charts, available at: <http://www.ukho.gov.uk> (last access: 20 May 2014), 2014. 6004
- USGS-EROS: Landsat data, US Geological Survey (USGS) Earth Resources Observation and Science (EROS). A combination of TM, ETM+ and OLI bands from 20 January 2001, 2014. 6046
- van Scheltinga, A. D. T., Myers, P. G., and Pietrzak, J. D.: A finite element sea ice model of the Canadian Arctic Archipelago, *Ocean Dynam.*, 60, 1539–1558, 2010. 5996
- van Scheltinga, A. D. T., Myers, P. G., and Pietrzak, J. D.: Mesh generation in archipelagos, *Ocean Dynam.*, 62, 1217–1228, doi:10.1007/s10236-012-0559-z, 2012. 6002, 6005, 6010, 6020, 6029
- Viré, A., Xiang, J., Milthaler, F., Farrell, P. E., Piggott, M. D., Latham, J.-P., Pavlidis, D., and Pain, C. C.: Modelling of fluid–solid interactions using an adaptive mesh fluid model coupled with a combined finite–discrete element model, *Ocean Dynam.*, 62, 1487–1501, 2012. 6017

Integration of GIS into meshing for geophysical models

A. S. Candy et al.

Title Page

Abstract

Introduction

Conclusions

References

Tables

Figures



Back

Close

Full Screen / Esc

Printer-friendly Version

Interactive Discussion



- Wang, Q., Danilov, S., Hellmer, H., Sidorenko, D., Schröter, J., and Jung, T.: Enhanced cross-shelf exchange by tides in the western Ross Sea, *Geophys. Res. Lett.*, 40, 5735–5739, 2013. 5996
- Wells, M. R., Allison, P. A., Piggott, M. D., Hampson, G. J., Pain, C. C., and Gorman, G. J.: Tidal modeling of an ancient tide-dominated seaway, Part 1: Model validation and application to global early cretaceous (aptian) tides, *J. Sediment. Res.*, 80, 393–410, doi:10.2110/jsr.2010.044, 2010. 6003
- Wessel, P. and Smith, W. H. F.: A global, self-consistent, hierarchical, high-resolution shoreline database, *J. Geophys. Res.*, 101, 8741–8743, doi:10.1029/96JB00104, 1996. 5997, 6002
- Wessel, P. and Smith, W. H. F.: New, improved version of generic mapping tools released, *Eos T. Am. Geophys. Un.*, 79, p. 579, doi:10.1029/98EO00426, 1998. 6000, 6006, 6011
- West, I. M.: *Geology of the Wessex Coast (including the UNESCO World Heritage Jurassic Coast and the Isle of Wight and part of East Devon)*, available at: <http://www.southampton.ac.uk/~imw> (last access: 20 May 2014), 2014. 6050, 6060
- Westerink, J., Luettich, R., Feyen, J., Atkinson, J., Dawson, C., Roberts, H., Powell, M., Dunion, J., Kubatko, E., and Pourtaheri, H.: A basin to channel scale unstructured grid hurricane storm surge model applied to southern Louisiana, *Mon. Weather Rev.*, 136, 833–864, 2008. 5995, 5997, 6002
- White, L., Deleersnijder, E., and Legat, V.: A three-dimensional unstructured mesh finite element shallow-water model, with application to the flows around an island and in a wind-driven, elongated basin, *Ocean Model.*, 22, 26–47, doi:10.1016/j.ocemod.2008.01.001, 2008. 5996, 6011
- Xi, Y. and Wu, J.: Application of GML and SVG in the development of WebGIS, *Journal of China University of Mining and Technology*, 18, 140–143, doi:10.1016/S1006-1266(08)60030-9, 2008. 6004
- Zorndt, A. C., Schlurmann, T., and Grabemann, I.: The influence of extreme events on hydrodynamics and salinities in the Weser Estuary in the context of climate impact research, *Coast. Eng. Proc.*, 1, doi:10.9753/icce.v33.currents.50, 2012. 5997

Integration of GIS into meshing for geophysical models

A. S. Candy et al.

Table 1. Summary of the different tasks and plugins developed. The latter two supplement standard GIS tools to aid mesh generation by the *boundary identification* and *mesh surface* processes.

Task	Description	Plugin developed
Identification of boundaries	Identifies physical boundaries and interfaces for reference in the numerical simulation code.	boundary identification
Mesh generation	Generation of a mesh on the enclosed surface defined by the boundary representation and constrained by a metric field. Additionally applies reference identification of the boundaries and interfaces defined by the above.	mesh surface
Field aggregation	For operations on, and the combination of, surface fields.	meshing raster calculator
Polygon rasterisation	Produces a surface field from a vector surface.	rasterise polygons

Title Page

Abstract

Introduction

Conclusions

References

Tables

Figures



Back

Close

Full Screen / Esc

Printer-friendly Version

Interactive Discussion



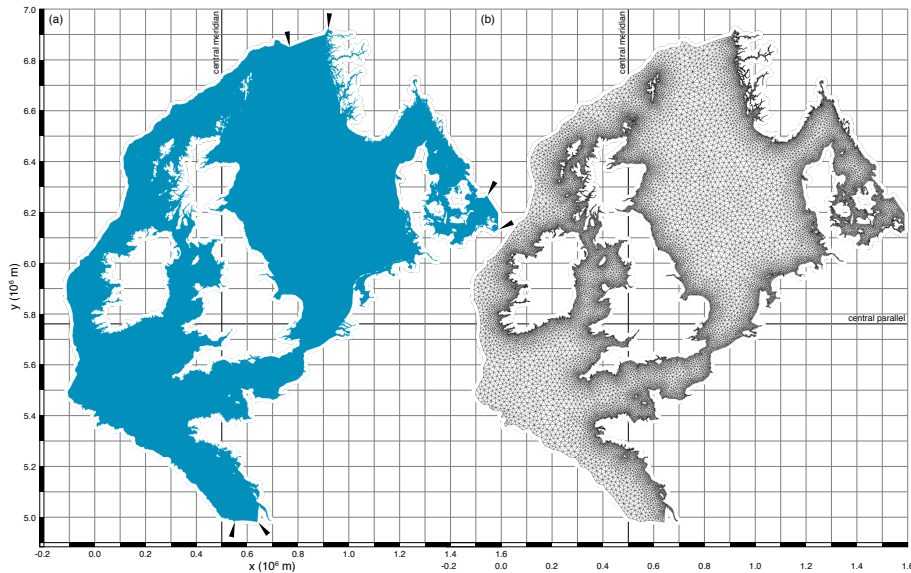


Figure 1. (a) The boundary representation on the surface geoid, constructed within a GIS framework; containing the British Isles, North Sea and coastline of northwest Continental Europe (filled for clarity). This surface is defined by a boundary representation developed from the intermediate resolution GSHHS contour, in combination with a bound marking the continental shelf-break. The latter is developed from an isobath of -300 m, shown in Fig. 2a. The two polylines are connected by straight lines, with the joins highlighted by black triangular markers. (b) The resultant mesh, generated by the Gmsh 2-D *MeshAdapt* algorithm, of the geoid surface defined in (a) under a simple metric based on the proximity to coastline. The characteristic element size ranges from 5 km within 1 km of the coast, to 20 km at 100 km into open waters to generate a mesh containing 24 794 nodes and 42 319 triangular elements. Both are plotted under a UTM projection in zone 30U.

Title Page

Abstract

Introduction

Conclusions

References

Tables

Figures



Back

Close

Full Screen / Esc

Printer-friendly Version

Interactive Discussion



Integration of GIS
into meshing for
geophysical models

A. S. Candy et al.

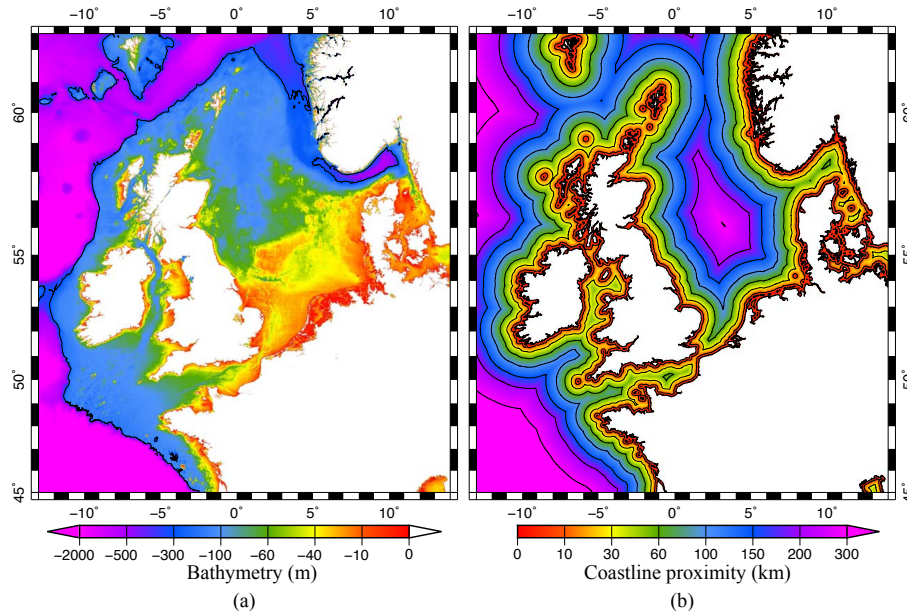


Figure 2. Development of mesh size metric from multiple datasets including: **(a)** ocean bathymetry, a raster surface map, and **(b)** proximity to coastline (i.e. the boundary representation identified as coastline and not open-ocean), a function from a parameterised vector path to a scalar field defined on the geoid surface. The latter is generated using GIS tools and further manipulated, in combination with **(a)**, to give a field suitable to apply as a element edge length metric presented in Fig. 3.

[Title Page](#)[Abstract](#)[Introduction](#)[Conclusions](#)[References](#)[Tables](#)[Figures](#)[Back](#)[Close](#)[Full Screen / Esc](#)[Printer-friendly Version](#)[Interactive Discussion](#)

Integration of GIS into meshing for geophysical models

A. S. Candy et al.

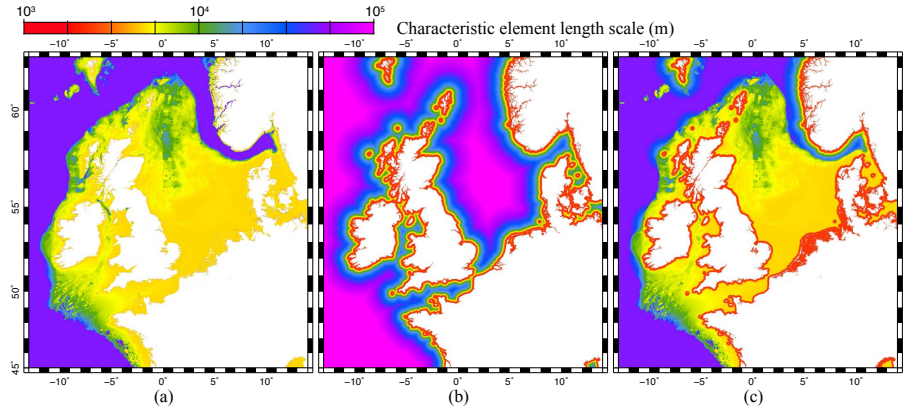


Figure 3. Characteristic element length scale metrics from the source fields presented in Fig. 2, generated with arithmetic operations within the GIS framework. The metric shown in **(a)** is a function of the bathymetry raster field of Fig. 2a described by Eq. (5). Correspondingly, **(b)** shows the function Eq. (6) of the proximity raster field Fig. 2b. These fields are combined in **(c)** following Eq. (4), that together with the boundary representation in Fig. 1 and boundary identification, are fed to the meshing tool to give the domain discretisation shown in Fig. 16.

[Title Page](#)[Abstract](#)[Introduction](#)[Conclusions](#)[References](#)[Tables](#)[Figures](#)[Back](#)[Close](#)[Full Screen / Esc](#)[Printer-friendly Version](#)[Interactive Discussion](#)

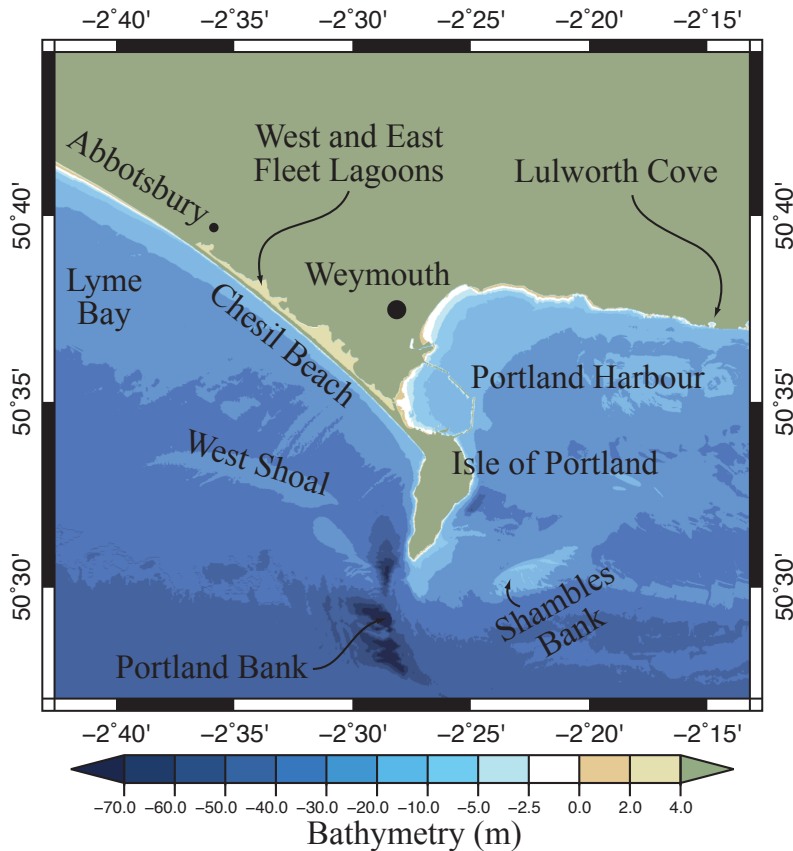


Figure 5. A bathymetry map of the region shown in Fig. 4b, under the same projection, with geologic and geographic features marked. Data comes from four tiles of the gridded Marine Digimap Coastal Bathymetry (Marine Digimap, 2008) with a 1 arcsecond grid (approximately 30 m cell size). The reference level of the depth data approximates to the lowest astronomical tide.

Integration of GIS into meshing for geophysical models

A. S. Candy et al.

Title Page	
Abstract	Introduction
Conclusions	References
Tables	Figures
◀	▶
◀	▶
Back	Close
Full Screen / Esc	
Printer-friendly Version	
Interactive Discussion	





Figure 8. An aerial photograph pre-2000 of Ferry Bridge at the mouth of the Fleet Lagoon that lies behind Chesil Beach, that itself can be seen in the bottom left of the image. Compare with Fig. 7a, where the boundary representation is developed using a combination of extracted polylines. Image courtesy of West (2014).

Integration of GIS into meshing for geophysical models

A. S. Candy et al.

Title Page

Abstract

Introduction

Conclusions

References

Tables

Figures

◀

▶

◀

▶

Back

Close

Full Screen / Esc

Printer-friendly Version

Interactive Discussion



Integration of GIS into meshing for geophysical models

A. S. Candy et al.

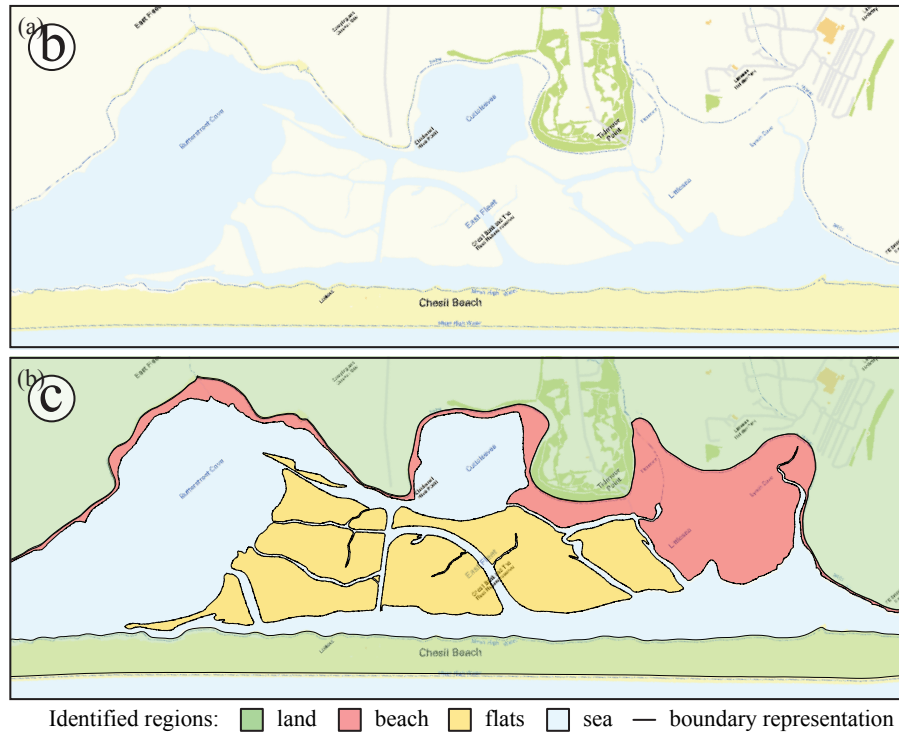


Figure 10. (a) A portion of the *OS Street View* SY67NW tile centred around the East Fleet region behind Chesil Beach, identified in Fig. 9. (b) The same region overlaid with vector polygon layers containing generated contours of the beach and flat regions, marked in red and yellow respectively.

Title Page

Abstract	Introduction
Conclusions	References
Tables	Figures
◀	▶
◀	▶
Back	Close
Full Screen / Esc	
Printer-friendly Version	
Interactive Discussion	



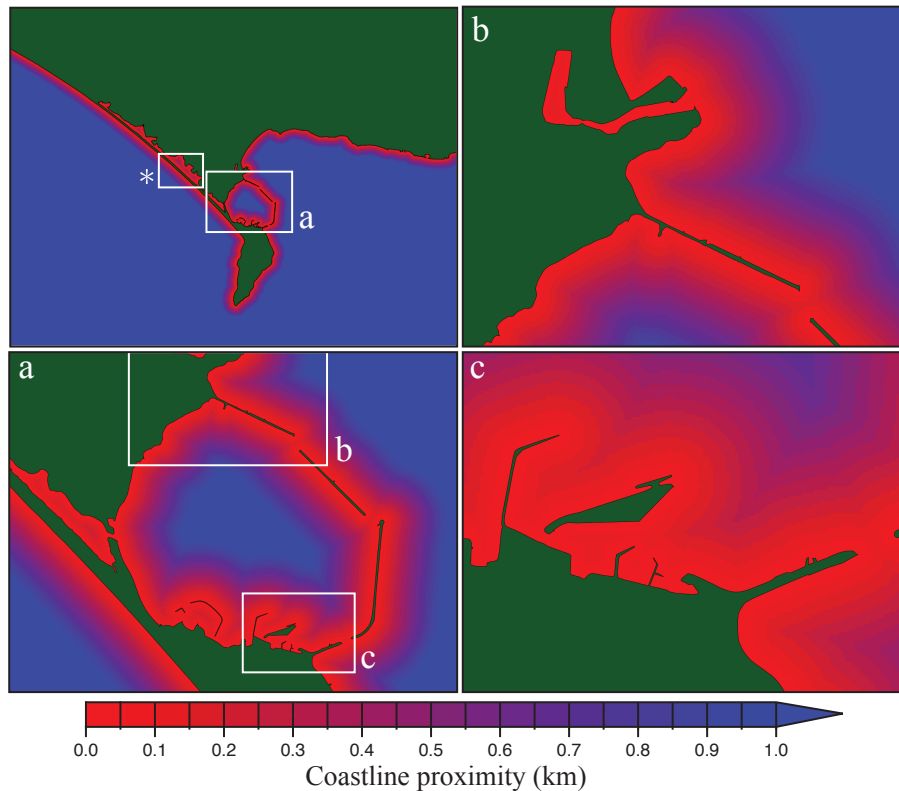


Figure 11. A metric field developed as a raster layer in GIS based on proximity to the main tidal boundary representation, that excludes the beach and flat regions. This form of metric enables the mesh to well-represent boundary representations, which can be particularly complex in ocean boundaries, where fractal-like coastlines bound the domain. This represents \mathcal{M}_c of Eq. (1). The box marked by * identifies the region shown in Fig. 12b.

Integration of GIS into meshing for geophysical models

A. S. Candy et al.

Title Page

Abstract Introduction

Conclusions References

Tables Figures

◀ ▶

◀ ▶

Back Close

Full Screen / Esc

Printer-friendly Version

Interactive Discussion



Integration of GIS
into meshing for
geophysical models

A. S. Candy et al.

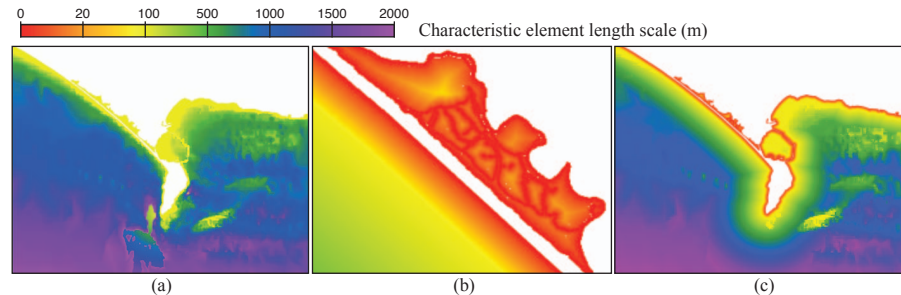


Figure 12. Development of the element edge length metric, constrained by multiple parameters and datasets. **(a)** Oceanic bathymetry metric from the fine-scale Digimap hydrospatial data shown in Fig. 5, following Eq. (2). **(b)** A metric based on a combination of proximity fields developed in Fig. 10, defined by \mathcal{M}_p in Eq. (1). The region marked by * in Fig. 11 is shown to highlight the proximity field in the vicinity of the East Flats. **(c)** Combined metric, with constraints from the fields derived from bathymetry and coastline location data.

Title Page

Abstract

Introduction

Conclusions

References

Tables

Figures

◀

▶

◀

▶

Back

Close

Full Screen / Esc

Printer-friendly Version

Interactive Discussion



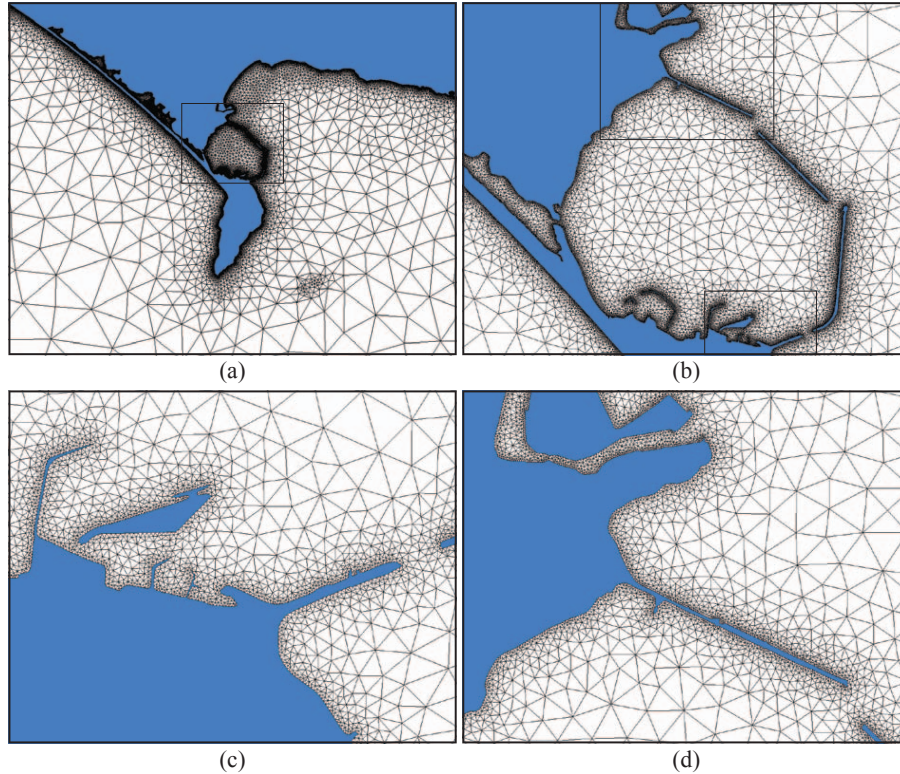


Figure 13. The mesh that results from a discretisation of the domain defined by the boundary representation defined in Figs. 7, 9 and 10b, combined with the metric field of Fig. 12c. Characteristic element length scales range from 5 m to 2 km in the regions shown here.

Integration of GIS into meshing for geophysical models

A. S. Candy et al.

Title Page	
Abstract	Introduction
Conclusions	References
Tables	Figures
◀	▶
◀	▶
Back	Close
Full Screen / Esc	
Printer-friendly Version	
Interactive Discussion	





Figure 14. Photograph of the man-made structures of Portland Harbour, for comparison with Fig. 13. Image courtesy of Portland Port (2014).

GMDD

7, 5993–6060, 2014

Integration of GIS into meshing for geophysical models

A. S. Candy et al.

Title Page

Abstract

Introduction

Conclusions

References

Tables

Figures



Back

Close

Full Screen / Esc

Printer-friendly Version

Interactive Discussion



Integration of GIS into meshing for geophysical models

A. S. Candy et al.

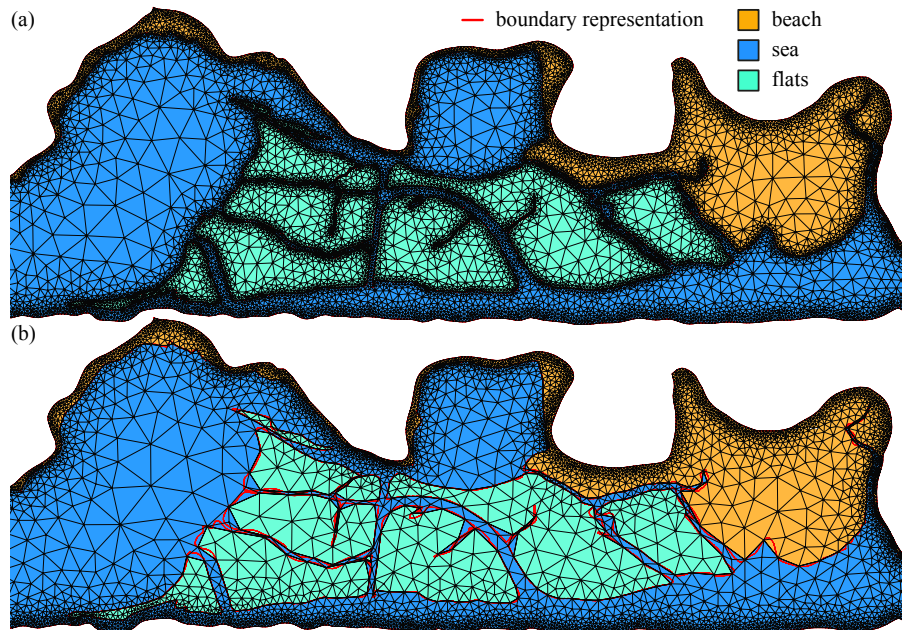
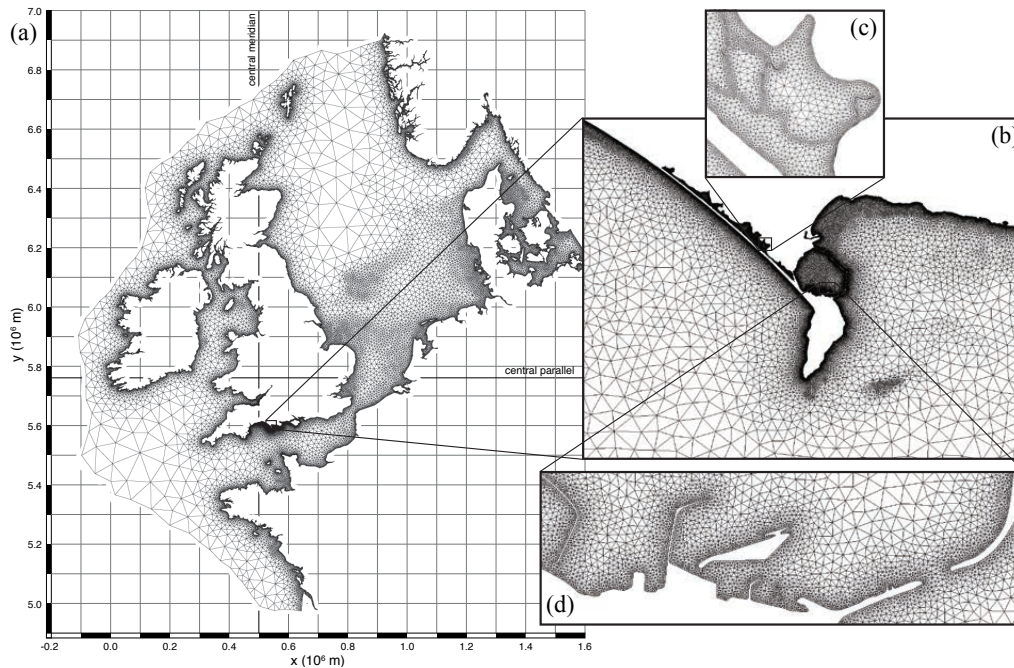


Figure 15. The meshed flats region centred around the East Fleet shown in Fig. 10a. Both are constrained by the metric Eq. (3), where $\gamma = \frac{1}{2}$ in **(a)** such that proximity to the internal boundary of the flats is given a weighting equal to the proximity to the coastline and $\gamma = \frac{1}{15}$ in **(b)**, with less weighting given to the representation of region boundaries. The characteristic element size ranges from 10 m at the coast to approximately 100 m inside the section of domain shown in both cases.

Integration of GIS into meshing for geophysical models

A. S. Candy et al.



Title Page

Abstract

Introduction

Conclusions

References

Tables

Figures



Back

Close

Full Screen / Esc

Printer-friendly Version

Interactive Discussion



